1. Proofread document received (18 - 09 -2021)

2. Submitted to
“the Journal of Asian Architecture and Building Engineering” (9 -9-2021)

3. Received from Reviewers (01-9-2021)

4. Revised manuscripts with special note (21-9-2021)

5. Revised manuscripts with highlights (21-9-2021)

6. Paper accepted (11-11-2021)

7. License Agreement (14-11-2021)

1. Proofread document received (18 - 09 -2021)

Harvesting Renewable Energies through Innovative Kinetic Honeycomb Facades: The Mathematical & CFD Modeling for Wind Turbine Design Optimization

Danny Santoso Mintorogo[1*], Aris Budhiyanto[1], Feny Elsiana[1], Fandi D. Suprianto[2], & Sutrisno[2]
[1]Department of Architecture, Petra Christian University
[2]Department of Mechanical Engineering, Petra Christian University
Siwalankerto street no. 121-131, East-Java, Indonesia
[*]Corresponding author; Email: dannysm@petra.ac.id

Abstract

The research was conducted on harvesting renewable energies through innovative kinetic honeycomb facades using micro-wind turbines, photovoltaics, and natural light pipes in buildings. It was specifically focused on the renewable energy factors associated with thousands of hexagonal micro-module wind turbines, hexagonal solar cell modules, and hexagonal modules for solar-reflecting pipes usually applied for deep sunlight reflection into a room of a building which has a veiled facade on the outside. This involved the utilization of windmills and solar cells specifically designed in a non-structural facade of the front building envelope through a double facade technique. Moreover, electrical energy was obtained from each windmill module while extra renewable electricity from abundant sunlight was acquired through the hexagonal modules of the solar cells (photovoltaic) designed vertically on the building facade. This means this current research only focuses on hexagonal wind turbines. Furthermore, ANSYS Fluent 12.0 simulated software and numerical analysis were used to optimize and redesign the wind turbine blades in order to obtain more electricity from one micro-module hexagonal wind turbine. The results showed that this design was able to produce 2.66 Watts per wind turbine compared to the 0.12 Watt from the previous design. The TSR was also found to be 0.5 and its power coefficient value (C_P) of 0.4525 was observed to be much higher than the 0.0343 from the previous design. This, therefore, means the architecture domain in multilevel buildings has the ability to harvest sustainable greenery energies from such a smart façade.

Keywords: Harvest renewable energy, kinetic honeycomb architectural façade, numerical and simulated CFD, wind turbines design for second façade architecture buildings.

1. Introduction

The world has been experiencing an extreme global energy crisis since 1979 due to the high need for energy (Manieniyen, 2009). Several countries have, therefore, been exploiting conservative biomass such as fossil fuels in the form of gasoline, coal, oil, propane, and natural gas. According to the United States Energy Information Administration (EIA), un-canopies natural energies are usually used and these include 80% from fossil fuels as indicated by 35,3% petroleum, 19,6% coal, and 26,6% natural gas while only 8,3% is from nuclear energy, and 9.1% from renewable energy (Coyle, 2014, p.15). Moreover, nuclear reactors currently use uranium (U), plutonium (Pu), and thorium (Th) as fuel to produce energy. This led to the search for eco-friendly environmental energies from hydrogen as the alternative gasoline in order to reduce CO2 pollution and asthma prevalence. There are other eco-friendly energy sources except hydro-energy and nuclear power and these include solar power or photovoltaics which involves using the abundant sun rays through solar radiation to generate electricity. The process involves installing either fixed or rotatable solar panels for approximately 10 hours on rooftops, canopies, or facades. Another alternative is the force-moving kinetic wind or wind turbines which generate electricity silently for almost 24 hours (Dudley, 2008, p.39). Biomass is another option through direct heating or biomass boilers and involves burning urban dry leaves or pruned trees as well as house and farm unused papers to generate energy while increasing household incomes and reducing city garbage (Nowak et al., 2019).

Style Definition ... [1]

Deleted: by …hrough Innovative Kinetic Honeycomb Facades: The Mathematical & CFD Modeling for Optimizing …ind Turbine Design ... [2]

Deleted: research, …esearch was conducted on harvesting renewable energies by …hrough innovative kinetic honeycomb facades with micro …sing micro-wind turbine…urbines, photovoltaics, photovoltaics …nd natural light pipes in buildings, will be focused … It was specifically focused on the renewable energy factors, where there will be factors associated with thousands of hexagonal micro-module wind turbines, hexagonal solar cell modules …odules, and hexagonal modules of solar …or solar-reflecting pipes usually applied for reflect sunlight …eep sunlight reflection into a room in …f a building which has a veiled facade outside a building…n the outside. Utilization …his involved the utilization of windmills and solar cells that are specifically designed in the … non-structural facade of the front building envelope (with …hrough a double facade technique)… From thousands of hexagonal windmill modules installed in the building facade…oreover, it will obtain electrical energy was obtained from each windmill module that is designed to be integrated with …hile extra renewable electricity from abundant sunlight was acquired through the building facade. Also equipped with …exagonal modules of the solar cells (photovoltaic) which will be …esigned vertically on a building facade to be able to support …he acquisition of extra renewable electricity from abundant sunlight in …uilding facade. This means this tropical country. The …urrent research this time will …nly focus …ocuses on hexagonal wind turbines. By using simulated software Furthermore, ANSYS Fluent 12.0 simulated software and numerical analysis on the research, the optimizing …ere used to optimize and redesign the wind turbine blades for obtaining …n order to obtain more electricity on …rom one micro-module hexagonal wind turbine could reach …urbine. The results showed that this design was able to produce 2.66 Watts per wind turbine than previous design of only compared to the 0.12 Watt per wind turbine module. Further, from the previous design. The TSR is …as also found to be 0.5 and the new …ts power coefficient value (C_P) of 0.4525 is …as observed to be much higher compare to previous design of C_P value 0.0343…han the 0.0343 from the previous design. The …his, therefore, means the architecture domain in multilevel buildings now can …as the ability to harvest sustainable greenery energies in ... [3]

Deleted: ; … kinetic honeycomb architectural façade; … numerical and simulated CFD; ... [4]

Deleted: In the decay the …he world has been suffered for experiencing an extreme global energy crisis extremely since 1979 due to humankind has always needed more …he high need for energy consumption …Manieniyen, 2009). Up till now, many …everal countries have tendered to exploit have, therefore, been exploiting conservative biomass such as fossil fuels known as …n the form of gasoline, coal, oil, propane, and natural gas. According to the United States Energy Information Administration (EIA), we often used un-canopies natural energies, …nergies are usually used and these include 80% of the total energy use gained …rom fossil fuels; the energy of petroleum is …uels as indicated by ... [5]

Renewable energies are becoming more important in cities and rural areas due to the high demand for energy in recent decades for residential and commercial purposes, especially in remote areas such as islands located very far from government power plants (Daryanto, 2007). Previous studies showed that 31% of energy is consumed through transportation while residential and commercial buildings use nearly 40%-42% (Cao, Xilei & Liu, 2016) and have the greatest total essential energy consumed in the U.S. and E.U (EIA, 2004b). Moreover, the Energy Efficiency Division of the Philippines Department of Energy (DOE) (2002) showed that 15 to 20% of the total national energy in the country was consumed by buildings and industries while a higher percentage of 66% was reported in California, USA (California Energy Commission, 2005). It was also predicted that the energy needed by this sector from different sources in countries which are not members of the Organization for Economic Cooperation and Development Countries (OECD) between 2010 to 2050 is expected to increase from 50 quadrillions BTU to approximately 32 - 82 quadrillion BTU while the value required by OECD members is expected to be from 7 quadrillions BTU to approximately 48 to 55 quadrillion BTU as indicated in Figure 1.

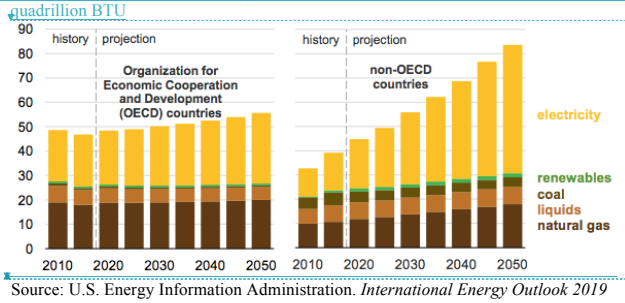

Source: U.S. Energy Information Administration. *International Energy Outlook 2019*

Figure 1. Energy Consumption in Buildings by Many Energy Resources (2010-2050)

This means more renewable energy is needed to generate and harvest sustainable electricity for residential and commercial or rental office buildings considering the small quantity it presently contributes when compared to the normal fossil oil as indicated in Figure 1. Countries of the world are observed to be constructing and consuming renewable energy, especially from solar and wind sources, as indicated by the annual average increase of 3.6% from 2018 to 2050 and a gradual decrease in coal-based energy consumption from 35% in 2018 to 22% at the end of 2050. This means coal is the current primary source while renewable energy is projected to contribute 50% of the total world electricity production in 2050 (International Energy Outlook, 2019). It is also important to note that Building Integrated Photovoltaics System (BIPV) through thousands of solar cells has also been installed across the world from 2013 to 2019 to generate around 5.4 GW and annual growth of 18.7% (Attoye, 2018).

The objective of this research was to propose and obtain renewable energies on building facades using honeycomb module wind turbines.

Deleted: Another reason to applying the renewable ... [6]

Deleted: quqdrillion british thermal units

Deleted:

Formatted: Font:Bold, Font color: Black

Deleted: Last reason to install or have …his means mor ... [7]

Deleted: research …bjective is …f this research was to ... [8]

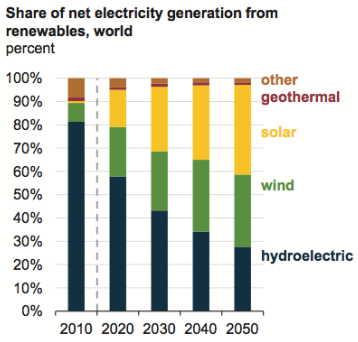

Source: U.S. Energy Information Administration. *International Energy Outlook 2019*

Figure 2. World Net Electricity Production from Renewable Sources (2010-2050)

2. Renewable Energy

The focus of this research is on renewable energy from solar and wind sources using a smart energy honeycomb façade. This façade depends on a double skin façade which has three parts which include the upper-part hexagonal module in the form of series of horizontal light pipes built on room ceilings to tap energy from daylight. The middle-part honeycomb module façades consist of thousands of micro-wind turbines to tap energy from kinetic wind sources while the bottom-part hexagonal modules include thousands of photovoltaic cells used to harness energy from solar radiation as indicated in Figures 3A and B.

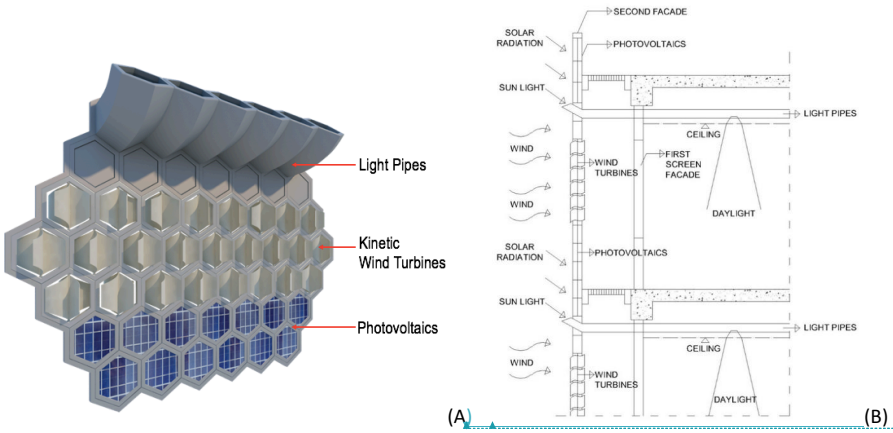

Figure 3. (A) Conceptual Double Skin Smart Façade (Light-Pipes, Wind Turbines, Photovoltaic Cells). (B) Schematic Building Section-Drawing showing features of light pipes, wind turbines, and photovoltaics.

2.1. Biomimicry Smart Façade Concept

The common double facade building technique applied has been reported to be very effective for energy conservation for a long period (Ahmed, 2016). It is also designed to save energy and assist in

Deleted: net
Deleted: Supplier
Deleted: paper will study
Deleted: coming
Deleted: energies on this
Deleted: The smart energy honeycomb
Deleted: relies
Deleted: the
Deleted: that consists to
Deleted: parts:
Deleted: is for energy coming from daylighting. It is
Deleted: to which the light pipes build
Deleted: the
Deleted: ceilings
Deleted: Middle
Deleted: are made up
Deleted: micro
Deleted: that are
Deleted: coming
Deleted: energy. Bottom
Deleted: are for
Deleted: coming
Deleted: that are thousands of photovoltaic cells (Figure 3 A & B)
Deleted:) ... [9]
Formatted: Font color: Black
Formatted: Font color: Black
Deleted:) (A
Deleted: light-
Deleted: turbines & photovoltaics (B)
Deleted: is
Deleted: in
Deleted: in the
Deleted: run
Deleted: , but this double kinetic façade designed
Deleted: not only saving
Deleted: but

the process of collecting renewable energies as a contribution to finding solutions to the world energy crisis. Moreover, the idea of using the honeycomb form or bio-mimicry was based on the (1) regular modular to represent the rigidity of the facade structure and 2) each hexagon module is filled with honey which serves as the source of life for children of bees known as larvae and the queen bees as indicated in Figure 4A. This design is projected to retrieve renewable electricity using thousands of small windmills placed in one-third of the smart facade as shown in Figure 4B while solar cells are on the lower part and the hexagon-shaped reflection pipes are at the top as indicated in Figure 3A.

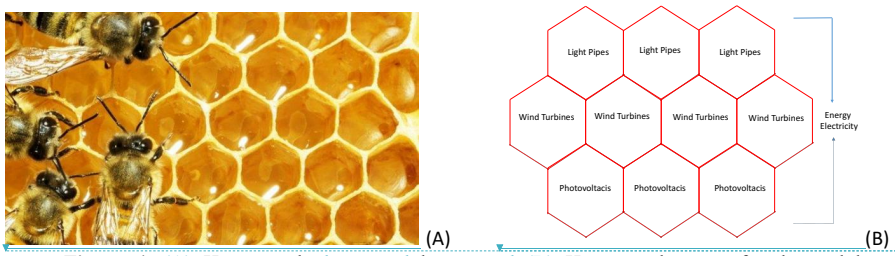

Figure 4. (A) Honeycomb, bees, and honey and (B) Honeycomb smart façade module and electricity

The term BIPV (Building Integrated Photovoltaic) is normally used to define buildings incorporated with PV circuits on the roof or envelope system. BIPV systems can be used to replace roofing, curtain walls, glazing, or special elements such as eaves or canopies. It is usually applied in the concept of green architecture as an energy-saving strategy through the utilization of solar radiation which is an environmentally friendly renewable energy source (Howells & Roehrl, 2012). Meanwhile, Building Integrated Wind Turbine (BIWT) is a building designed using wind turbines in the facades to produce energy (Arteaga-López, Ángeles-Camacho, & Bañuelos-Ruedas, 2019).

2.2. Renewable Wind Turbines Energy Systems

An example of renewable energy from wind is the windmill which can be divided into horizontal and vertical types. These two types have the same mechanism and this involves the wind moving the propeller which later drives the motor to produce electrical energy but the difference is observed from the placement of the quite heavy motor. It is, however, important to note that the vertical type is more advantageous due to its ability to match the weight of gravity which is straight down. Moreover, the movement of the propeller on the wind turbine due to kinetic energy as the wind pushes its surface depends on its horizontal or vertical placement. This classification was also observed in the rotation of the shaft as indicated by the one rotating vertically when the rotor is located in a horizontal position as well as the horizontal rotation when the rotor was placed vertically which has been further developed into Savonius, Darrieus, and H-Rotor as indicated in Figure 5A.

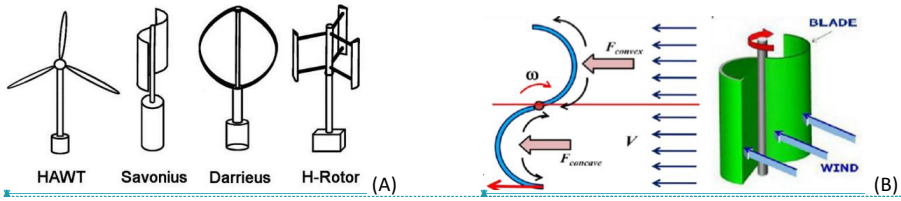

Figure 5. Horizontal and Vertical Rotating Propeller Placement (A) Principles of Wind Turbine Movement in the Savonius System (B)

Deleted: also …s a contribution to finding solutions t… [10]

Deleted:

Deleted:

Deleted: bees & …ees, and honey (A), …nd (B) Hone… [11]

Deleted: that use …ncorporated with PV circuits … [12]

Deleted: One of …n example of renewable energy wi… [13]

Deleted:

Formatted: Font:(Default) Times

Deleted:

Formatted: Font:(Default) Times

The wind turbine spins due to the difference in pressure on each blade. For example, one of the sunken sides of the Savonius vertical wind turbine captures the wind and spins it while the other side of the convex receives also wind and causes the turbine to spin as shown in Figure 5B (Wenehenubun, Saputra, & Sutanto, 2015). It is possible to turn the wind turbines in tall buildings over using two systems. The first involves using several large wind turbines placed on the roof of a building, between two adjacent buildings, or in a hole created inside the building as indicated in Figure 6A and this design can be found in the World Trade Center building in Bahrain. The second method is using many small wind turbines installed on buildings as showed in Figure 6B and this is considered advantageous due to the fact that the size of the turbines reduces its ability to overload the building structure but requires to be installed in high number to produce the energy needed. An example of these designs can be found in the Miami Coral Tower in Miami (Park, Jung, Lee, & Park, 2015). Meanwhile, Savonius VAWT (S-VAWT) is a good candidate due to its high initial torque, low cost, easy installation and repair, and sturdiness (Manwell et al., 2010, 1-3).

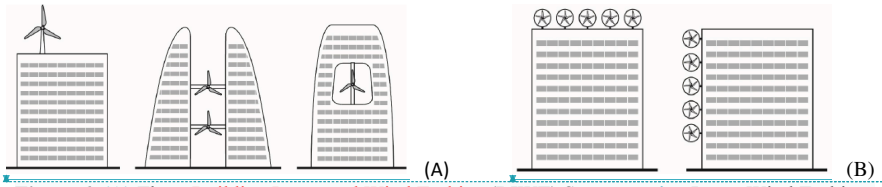

Figure 6. (A) Three Building Integrated Wind Turbine (BIWT) Systems using Large Wind Turbines and (B) Two BIWT Systems Use Small Sized Wind Turbines. (Source: Park, 2015).

3. Methodology Overview

The purpose of this research was to obtain the maximal values of electrical power from wind turbines' hexagonal frame smart façade module. It was focused on redesigning the wind turbine blades numerically after which they were simulated using ANSYS Fluent which is a simulation computational fluid dynamic (CFD) analysis program.

The previous experimental design of the Savonius wind turbine with 4 blades was used as the basis for the experimental model tested in the wind tunnel at the Mechanical Engineering laboratory and the Cp was found to be only 0.003426. Meanwhile, one module of hexagonal windmill produced 2.30 Volts, 0.05 Ampere, and 0.1182 Watt when the wind speed was 4 m/s while the values were 3.39 Volts, 0.01 Amperes, and 0.0607 Watt at 5 m/s (Mintorogo, 2019).

3.1. Shape and Size of Integrated Windmills in the Building Façade

The facade in the building has a small windmill dimension known as a micro wind turbine with the longest diameter being 0.30 meters while the shortest was 0.25981 meters. Moreover, the total area of the hexagons was 0.0585 m2 as indicated in Figure 7A. The "Savonius" Windmill was selected based on the consideration that it is the simplest method and works based on the differences in shear force or differential drag windmill as shown in Figures 7B and C.

Deleted: because there is a …ue to the difference in p[... [14]]

Deleted:

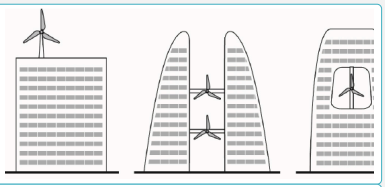

Deleted:

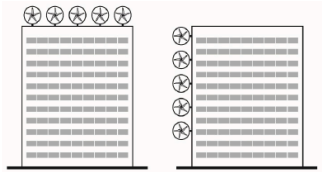

Formatted: Font color: Black

Formatted: Font color: Black

Deleted: Use …sing Large Wind Turbines (A) [... [15]]

Deleted: Turbines (B)

Deleted: of …rom wind turbines …urbines' hexagona[... [16]]

Deleted: Based on …he previous experimental design[... [17]]

Deleted: Windmill …he facade in the building with …[... [18]]

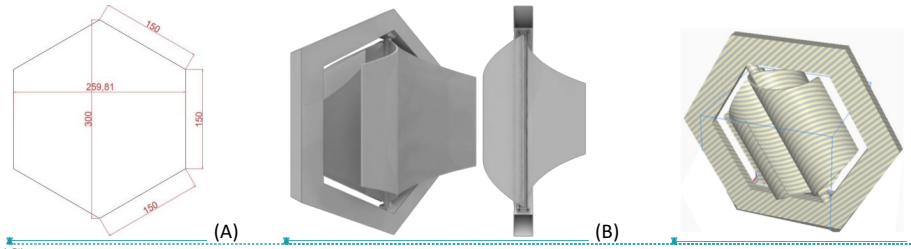

Figure 7. (A) Dimension of Honeycomb Windmill module, (B) Previous Design of Savonius Wind Turbine model, and (C) Optimized Savonius Wind Turbine Module with 4 Blades

3.2. Basic Theory for the Wind Turbine

Turbines are devices used in converting kinetic energy from the wind into motion energy. The amount of energy or turbine power (P) can theoretically be written as follows:

$$P = T\omega P = T\omega \quad (1)$$

Where:
P = Turbine power $(watt)(watt)$.
T = Torque or moment of the turbine $(Nm)(Nm)$.
ω = Angular velocity of the turbine (*rad/s*).

The area passed by the air was designed to have the same boundary end to the end and used as a reference value in the ANSYS Fluent 12.0 to determine the moment coefficient. Meanwhile, the dimensionless moment coefficient in line with Rahman et al. (2018, 13) is, therefore, stated as follows:

$$C_m = \frac{T}{\frac{1}{4}\rho A D V^2} C_m = \frac{T}{\frac{1}{4}\rho A D V^2} \quad (2)$$

Where:
$C_m C_m$ = Moment coefficient.
$\rho\rho$ = Fluid density (kg/m^3).
AA = Turbine blade cross-sectional area $(m^2)(m^2)$.
D = Diameter of the turbine $(m)(m)$.
V = Fluid velocity (m/s).

The aerodynamics in turbines also consist of several forces known as dimensionless forces such as the density and speed of the freestream body. The relationship between these two values is, however, expressed as dynamic pressure and represented using the following equation.

$$q_\infty = \frac{1}{2}\rho_\infty {V_\infty}^2 q_\infty = \frac{1}{2}\rho_\infty {V_\infty}^2 \quad (3)$$

Deleted:
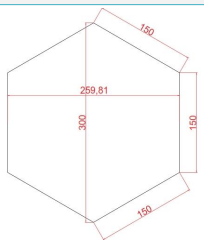

Formatted: Font:(Default) Times

Deleted:
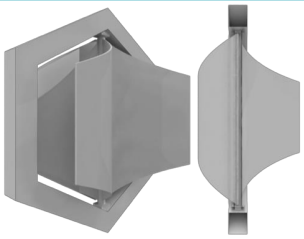
Formatted: Font:(Default) Times

Deleted:
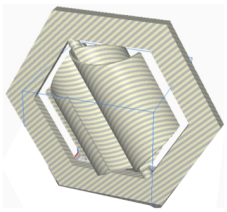
Formatted: Font:Times New Roman, Font color: R,G,B (34,34,34)

Deleted: module (A); .

Deleted: model (B); Optimazing New …odel, and (C) ... [19]

Deleted: for …sed in converting kinetic energy from t ... [20]

Deleted: is made …as designed to have the same from ... [21]

Deleted: .

Deleted: In addition to the moment coefficient, …he ... [22]

This means it is possible to define the dimensionless force as follows:

Lift coefficient: $C_L = \frac{L}{q_\infty S} C_L = \frac{L}{q_\infty S}$

Drag coefficient: $C_D = \frac{D}{q_\infty S} C_D = \frac{D}{q_\infty S}$

Normal force coefficient: $C_N = \frac{N}{q_\infty S} C_N = \frac{N}{q_\infty S}$

Axial force coefficient: $C_A = \frac{A}{q_\infty S} C_A = \frac{A}{q_\infty S}$

Where:

L = Lifting force $(N)(N)$

D = Drag force $(N)(N)$

N = Normal force $(N)(N)$

A = Axial force $(N)(N)$

S = Extensive reference area $(m^2)(m^2)$

The S or reference area in the coefficient was selected based on the shape of the body geometry and the values for different shapes are presented in Table 1.

Table 1. Cd values for different body shapes

Deleted: So,

Deleted: can be stated

Deleted: In the coefficient above, the value of

Deleted: (

Deleted: area) is chosen

Deleted: geometry,

Deleted: shapes, there

Deleted: different S values (table 1)

Deleted: various

Type of Body		Length Ratio	Re	C_D
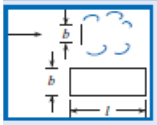	Rectangular plate	$l/b = 1$ $l/b = 5$ $l/b = 10$ $l/b = 20$ $l/b = \infty$	$>10^4$ $>10^4$ $>10^4$ $>10^4$ $>10^4$	1.18 1.20 1.30 1.50 1.98
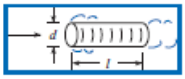	Circular cylinder with axis parallel to flow	$l/d = 0$ (disk) $l/d = 0.5$ $l/d = 1$ $l/d = 2$ $l/d = 4$ $l/d = 8$	$>10^4$ $>10^4$ $>10^4$ $>10^4$ $>10^4$ $>10^4$	1.17 1.15 0.90 0.85 0.87 0.99
	Square rod	∞	$>10^4$	2.00
	Square rod	∞	$>10^4$	1.50
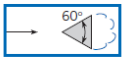	Triangular cylinder	∞	$>10^4$	1.39
	Semicircular shell	∞	$>10^4$	1.20
	Semicircular shell	∞	$>10^4$	2.30
	Hemispherical shell		$>10^4$	0.39
	Hemispherical shell		$>10^4$	1.40
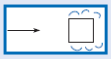	Cube		$>10^4$	1.10
	Cube		$>10^4$	0.81
	Cone—60° vertex		$>10^4$	0.49
	Parachute		$\approx 3 \times 10^7$	1.20

(Source: Elger et al., 2015, 371–372)

It is possible to capture some of the kinetic energy passing through the turbine cross-section and this is expressed as the power coefficient (Cp) which can be calculated using the following formula:

$$C_p = \frac{P}{\frac{1}{2}\rho A D V^3} = \frac{T\omega}{\frac{1}{2}\rho A D V^3} = \lambda C_m \qquad (4)$$

Deleted: A handful

Deleted: can be captured. This value

Deleted:). Cp value is

Deleted: by

Where:
C_p = power coefficient
P = power of the turbine (Watt).

The power coefficient of this turbine, however, depends on the Tip-Speed Ratio (TSR) which is the ratio of blade speed at the tip to the speed of airflow as indicated in the following relationship:

$$\lambda = \frac{\omega R}{V} \lambda = \frac{\omega R}{V} \quad (5)$$

Where:
$\lambda\lambda$ = Tip-speed ratio
RR = Turbin radius $(m)(m)$

The theoretical power coefficient limit is 0.59 and this is known as the Betz Limit. Meanwhile, Figure 8 shows the maximum value of the power coefficient (C_pC_p) against TSR for different types of turbines (Kumar & Saini, 2016, 293)

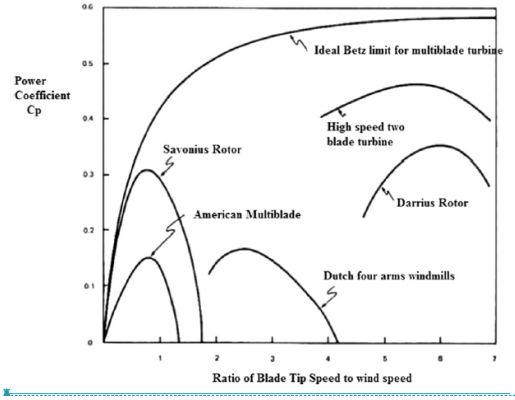

Figure 8. Power Coefficient against TSR

3.3. Simulation Validation

The validation process was conducted using a 3D model in accordance with Ferrari et al. and this involved the Savonius turbine model being in line with the Rotor C geometry [Ferrari, 2017]. Moreover, the Reynolds number used was based on turbine diameter (Dt) and bulk velocity (U_{inf}) which was 4.32 105 while the wind tunnel was in line with the method applied by Blackwell et al., and the 1.4% Turbulence Intensity used was in accordance with 1% recommended by Suchde et al. (2017, 255). The two simulations conducted with the experimental results of Blackwell et. al. 1977 in the wind tunnel showed that the most optimal Savonius turbine was found at approximately TSR 0.85 with a maximum Coefficient of power (Cp) value of 0.25 as indicated in Figure 9. The other TSR variables used based on the angular velocity of the rotor turbine include 0.576, 0.804, and 1.002 while the coefficient of power value was used for comparison. Moreover, the experimental trend of the Savonius turbine performance was presented through the simulation conducted using Ansys Fluent 16.0 with 3D Dimensional, Double

Deleted:
Meanwhile, the
Deleted: turbine …urbine, however, depends on the T... [23]
Deleted: 59. This limit
Deleted: various
Deleted:
Formatted: Font:(Default) Times New Roman
Deleted: Validation
Deleted: carried out with …onducted using a 3D mod... [24]

Precision, Pressure-Based Solver, Steady-State Condition, and Criteria Convergency 10-5. The Cell Zone conditions were also divided into static and dynamic frames with the dynamic conditions specifically having the frames of motion with rotational velocity.

The simulation results were compared with the Ferrari et al. findings and this study was discovered to have a smaller Cp due to its use of a mathematical model approach which led to some flow phenomena such as the turbulent flow which was observed to have been developing continually up to the present moment. Sutrisno et al. (2015) reported turbulence intensity as an energy reserve being converted gradually to flow and this means the flow with high turbulence tends to have stronger energy. Meanwhile, another flow phenomenon known as the swirl flow was reported by Simanjuntak et al. (2019) to have the capability to be used as a major factor in the coal drying process due to its ability to separate steam vapor in soil coal. The Savonius turbine simulation, however, used very strong turbulence and swirl flow phenomena, thereby, causing high uncertainty.

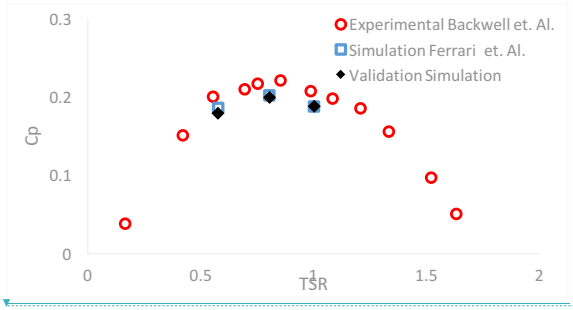

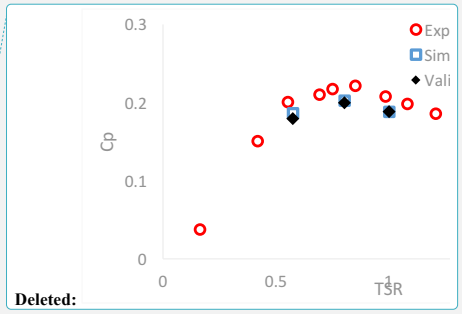

Figure 9. Comparison between the simulation results of Ferrari et al. and Blackwell et al.

The validation results showed large error values of 10.45%, 10.02%, and 9.43% at TSR 0.576, 0.804, 1.002 respectively as presented in Table 2. This means the model was unable to produce better predictions than Ferrari et al.'s prediction of the experimental results of Blackwell et al due to its use of a steady-state condition. It was, therefore, recommended that the unsteady state simulation approach which requires resource computation with high-performance equipment be used in further studies. Meanwhile, some other parameters were selected for the next process which involved optimizing the hexagonal turbine design. This validation method only compares one parameter due to the focus of this study on the optimization of a new design for the Savonius turbine shape.

Table 2. Comparison of the simulation validation result with the experiment of the Blackwell et al. (1977).

TSR	Simulation Validation	Error % Cp with Experiment Blackwell et al.
0.576	0.1791	10.45
0.804	0.1994	10.02
1.002	0.1883	9.43

4. RESULTS and DISCUSSION

Deleted: Pressure …ressure-Based Solver, Steady …t [25]

Deleted: two …imulation results between …ere comp [26]

Deleted:

Deleted: Simulation Result with Simulation …etween [27]

Deleted: results of this simulation …alidation show … [28]

Deleted: result validation …imulation validation resul [29]

Deleted: Validation Simulation

Deleted: Blackweel et.

The software used for simulation was ANSYS FLUENT 16.0 using the following parameters:
Viscous model: RNG k-epsilon, Standard Wall Function.
Rotational velocity: varied to obtain a different TSR
Velocity inlet : 4 m/s
Turbulent method: Intensity and length scale
Turbulent length scale: 0.001 m
Turbulent intensity : 5 % depend on wind tunnel
3D model & meshing: gambit software

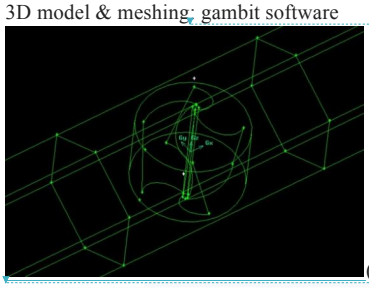
(A)
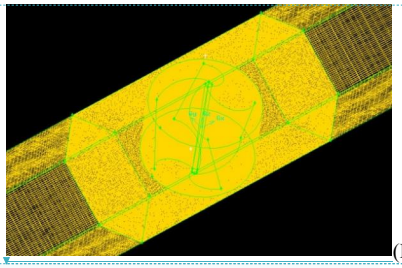
(B)

Figure 10. (A) Savonius 3D facet 3D model and (B) Savonius 3D meshing model

There is a variation in the radius, offset, and twist of the hexagonal or honeycomb wind turbine blades used. The simulation was conducted to obtain the value of the Power Coefficient for the Savonius hexagonal wind turbine using 6 radii which include 57.5 mm, 58 mm, 60 mm, 64 mm, 72 mm, and 87.4 mm as showed in Figure 11A, 5 offsets including 0 mm, 5 mm, 7 mm, 9 mm, and 11 mm as indicated in Figure 11B, and the 5 twist models including 0^o, 30^o, 45^o, 60^o, and 90^o as presented in Figure 11C. The design was simulated until the results converge. Moreover, a Y + check was also performed and the value was discovered not to exceed 500 (Tahani et al., 2016, 464) while flux conservation at the inlet and outlet also produced values below 1% and these were considered to be good (Suchde et al., 2017, 255).

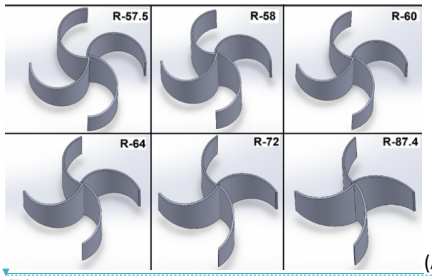

(A)
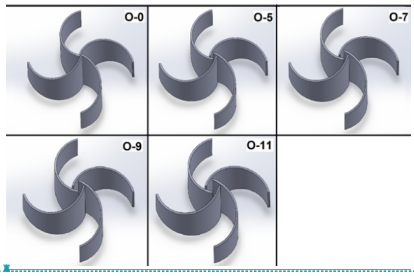

(B)

Deleted: is …as ANSYS FLUENT 16.0, and … using [30]
Deleted:
Deleted:
Deleted:
Deleted:
Deleted: on
Deleted:
Deleted:
Deleted:
Deleted: (A), …nd (B) Savonius 3D meshing model ([31]
Deleted: The model …here is a variation in the radius [32]
Deleted:
Deleted:
Formatted: Font:Times New Roman, 12 pt

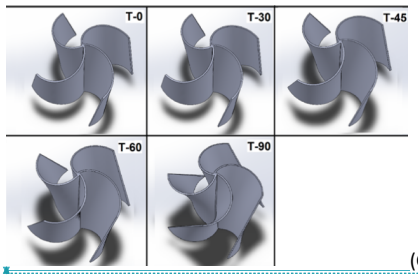

(C)

Figure 11. (A) Variation in the radius of the turbines, (B) Variation in Offset of the turbines, and (C)Variations in Twist of the turbines

Table 2 and Figures 12A and B showed the optimal value of the turbine blade was found at 58 mm radius with 0.5 TSR which produced 2.84 watts of power and torque of 0.099 Nm as indicated in Table 3 while the power coefficient (Cp) was 0.2786. The model of flow and turbulence kinetic energy produced are presented in 11A and B.

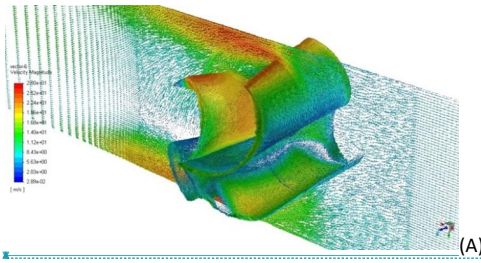

(A)

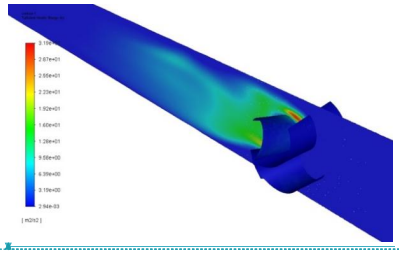

(B)

Figure 12. (A) Vector velocity of wind flow on a 58 mm radius turbine and (B) turbulent kinetic energy in a 58 mm radius turbine

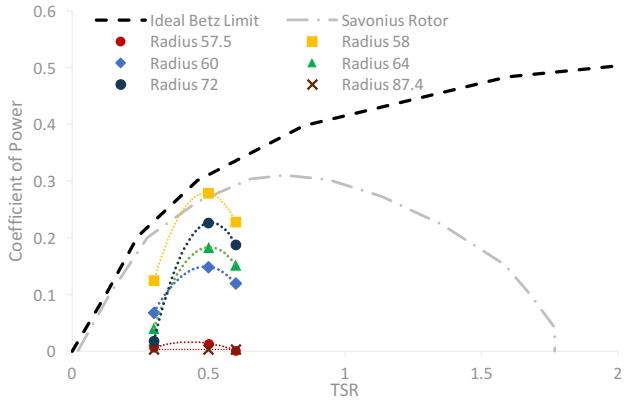

Deleted:

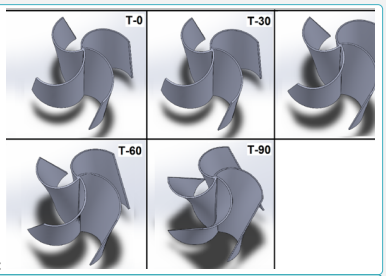

Formatted: Font:Times New Roman, 12 pt

Deleted: turbines (A), …urbines, (B) Variation in Off ... [33]

Deleted: (C)

Deleted: From the table …able 2 and figure 12 A & B ... [34]

Deleted:

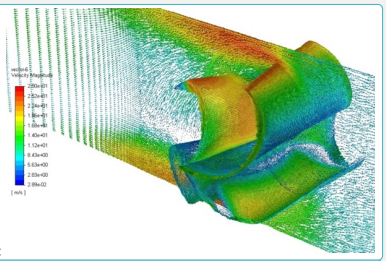

Deleted:

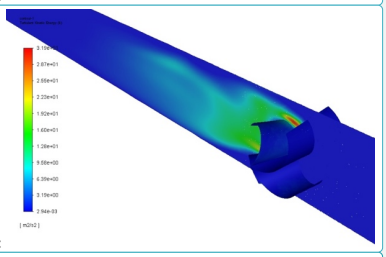

Deleted:

Formatted: Font:Times New Roman

Formatted: Font:Times New Roman

Deleted: (A),

Deleted: Count of …turbulent kinetic energy in a 58 r ... [35]

Figure 13. Variants of Turbine Blade Radius

Figure 13 shows the three models with 58 mm, 64 mm, and 72 mm radius, and the highest C_P values have the same flow velocity patterns. It was also discovered that a smaller drag flow was produced when the radius was fixed and this is less favorable for the performance of the turbine. Moreover, a larger radius produced a larger counter-rotating-vortices flow which is also less favorable for performance due to its smaller overlap flow. However, the greatest turbulent kinetic energy distribution in the rotor was found in turbines with the smallest diameter which was 58 mm. This means a larger diameter of the rotor produced the smaller distribution of turbulent kinetic energy as presented in Figure 12B.

Table 3. Variations in Turbine Blade Radius

Radius (mm)	TSR	C_P	Power (Watt)	Torque (N.m)	Y Plus
57.5	0.3	0.0063	0.01414182	0.001355268	83.13049
	0.5	0.01362	0.138701848	0.004817709	132.4085
	0.6	0.00102	0.006001218	0.000208448	112.7113
58	0.3	0.12423	0.278864743	0.026724749	85.26819
	0.5	0.2786	2.837076273	0.098543809	132.8681
	0.6	0.22797	1.338171874	0.04648044	112.3835
60	0.3	0.06798	0.152605393	0.014624799	88.38058
	0.5	0.14847	1.511890424	0.052514429	134.181
	0.6	0.11964	0.702281366	0.02439324	113.8718
64	0.3	0.04071	0.091376894	0.008757022	94.81096
	0.5	0.18333	1.866906431	0.064845656	144.2127
	0.6	0.15165	0.890188959	0.030920075	122.4319
72	0.3	0.01791	0.040192929	0.003851853	102.9334
	0.5	0.22628	2.304257532	0.080036733	156.9534
	0.6	0.18799	1.10346569	0.038328089	133.3397
87.4	0.3	0.00319	0.007153723	0.000685571	111.8106
	0.5	0.00312	0.031819299	0.001105221	184.3163
	0.6	0.00266	0.015604645	0.000542016	156.7907

Table 4 and Figures 14A and B show the optimal value of the turbine blade was produced at 11 mm offset with 0.5 TSR as indicated by the production of 3.05 watts of power, 0.106 Nm of torque, and 0.29918 power coefficient (C_P). The model of flow and turbulence kinetic energy produced are presented in Figure 13B.

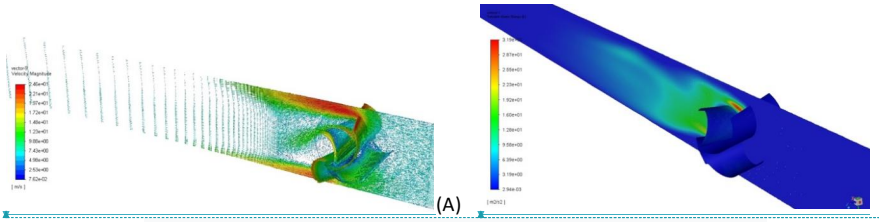

Figure 14. (A) Vector velocity of wind flow on an 11 mm offset turbine, and (B)turbulent kinetic energy in turbine offset 11 mm

Deleted: Varians

Deleted: The picture …igure 13 can be seen that …ho ... [36]

Deleted: Result of

Deleted: From table …able 4 and figure 14 A & B, it ... [37]

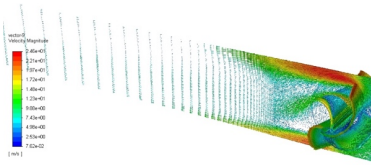

Deleted:

Formatted: Font:Times New Roman

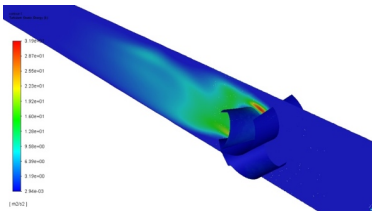

Deleted:

Formatted: Font:Times New Roman

Deleted: turbine (A), ... [38]

Deleted: (B)

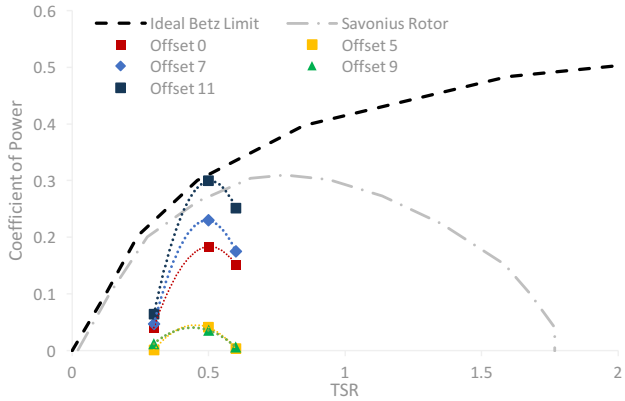

Figure 15. Variants of Turbine Blade Offset (Source: Author)

Figures 15 showed the three models with 11, 7, and 0 offsets with the highest C_P values have almost the same flow velocity patterns. A smaller drag flow was produced when the offset was reduced and this is less favorable to the performance of the turbine and the same was also observed for smaller offsets which caused a greater counter-rotating-vortices flow and smaller overlap flow. Meanwhile, the greater offset of the rotor was observed to cause smaller distribution of turbulent kinetic energy before it increased again.

Table 4. Variations in Turbine Blade Offset

Offset (mm)	TSR	C_P	Power (Watt)	Torque (N.m)	Y Plus
0	0.3	0.04071	0.091377	0.008757	94.81096
	0.5	0.18333	1.866906	0.064846	144.2127
	0.6	0.15165	0.890189	0.03092	122.4319
5	0.3	0.00095	0.002122	0.000203	87.08589
	0.5	0.04072	0.414702	0.014404	132.0764
	0.6	0.00335	0.019688	0.000684	112.0743
7	0.3	0.04683	0.105127	0.010075	84.6218
	0.5	0.22955	2.337588	0.081194	128.1884
	0.6	0.17445	1.023987	0.035567	108.7234
9	0.3	0.01217	0.027321	0.002618	82.36165
	0.5	0.03606	0.367162	0.012753	124.5991
	0.6	0.00611	0.035872	0.001246	105.5825
11	0.3	0.06421	0.144118	0.013811	80.24362
	0.5	0.29918	3.046607	0.105822	121.2431
	0.6	0.250932	1.472946	0.051162	102.7176

Table 4 and Figure 16 show that the optimal value of the turbine blade was at 0-degree twist with 0.5 TSR which produced 4.75 watts of power, 0.165 Nm of torque, and 0.4665 of power coefficient. The model of the flow and turbulence kinetic energy produced is presented in Figure 16B.

Deleted: Varians
Deleted: From pictures 15, it can be seen that
Deleted: (offset
Deleted: 7
Deleted: 0) have
Deleted: that
Deleted: patterns that are close to the same
Deleted: When
Deleted: is
Deleted: the resulting drag flow
Deleted: smaller, which is
Deleted: for
Deleted: turbine. For
Deleted: offsets, it produces
Deleted: counter
Deleted: flow, which is also less favorable for the performance of the turbine. A
Deleted: offset also results in smaller
Deleted: so this is also less favorable for turbine performance. The
Deleted: the
Deleted: in the rotor,
Deleted: the
Deleted: energy, then enlarges
Deleted: . The next test is to vary the turbine blade twist and get the following results in picture 16
Deleted: Result of
Deleted: The next test is to vary the turbine blade twist (picture 16). From table 4, it can be seen
Deleted: twist is
Deleted: 0
Deleted: TSR 0.5. In this condition the turbine can produce
Deleted: power and
Deleted: . The value of the power coefficient obtained is 0.4665
Deleted: of
Deleted: can be seen
Deleted: the pictures below (figure
Deleted:)

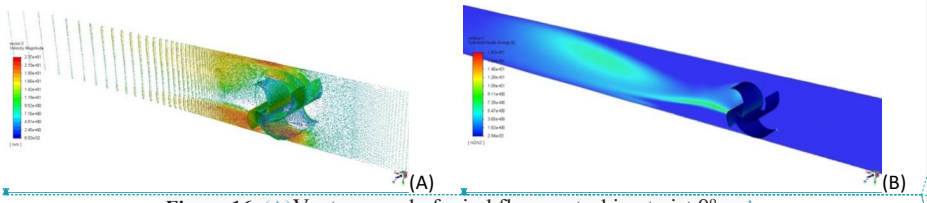

Figure 16. (A)Vector speed of wind flow on turbine twist 0° and (B) turbulent kinetic energy in turbine twist 0°

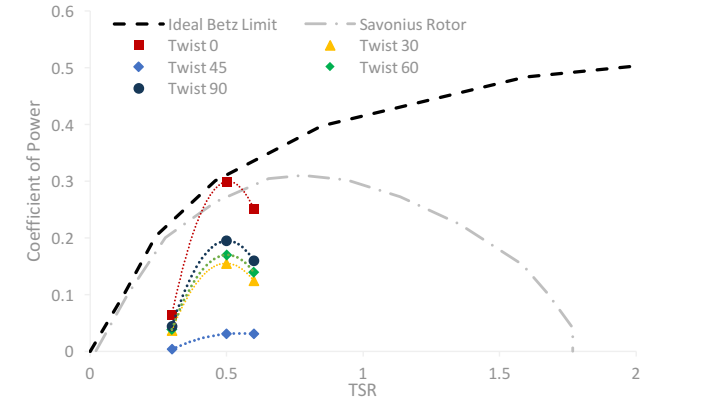

Figure 17. Variants of Turbine Blade Twist

Figure 17 shows the three models 0, 90, and 60 twists with the highest C_P values have almost the same flow velocity patterns. It was discovered that the minimized twist produced a smaller drag flow, and this is less favorable for the performance of the turbine due to its larger counter-rotating-vortices flow. A bigger twist also caused smaller overlap flow which is also considered less favorable and this means a greater twist of the rotor usually leads to a higher distribution of turbulent kinetic energy before the distribution shrinks again.

Table 5. Variations in Turbine Blade Twist

Twist (degree)	TSR	C_P	Power (Watt)	Torque (N.m)	Y Plus
0	0.3	0.06421	0.144118	0.013811	80.24362
	0.5	0.29918	3.046607	0.105822	121.2431
	0.6	0.250932	1.472946	0.051162	102.7176
30	0.3	0.0367	0.082452702	0.00790178	73.73257
	0.5	0.15497	1.578151371	0.054815956	113.7554
	0.6	0.12406	0.728239091	0.025294862	97.44502
45	0.3	0.00339	0.007624782	0.000730714	74.97164

Deleted:

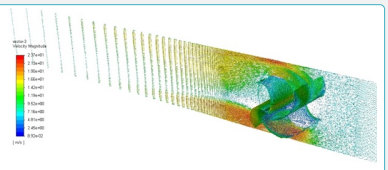

Deleted:

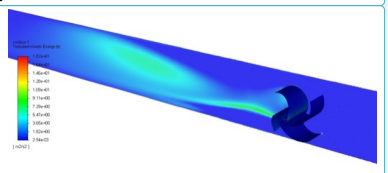

Deleted:

Formatted: Font:Times New Roman, 12 pt

Formatted: Font:Times New Roman, 12 pt

Deleted: (A),

Deleted: Count of …B) turbulent kinetic energy in tur … [39]

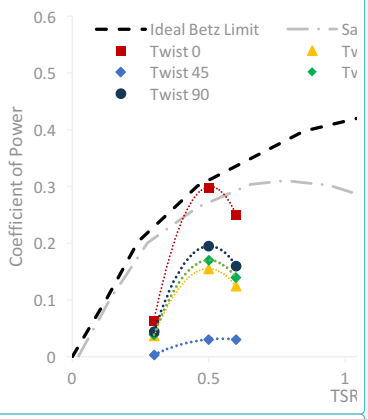

Deleted:

Deleted: From …igure 17 shows the picture 17, it can … [40]

Deleted: Result of

Twist (degree)	TSR	C_P	Power (Watt)	Torque (N.m)	Y Plus
	0.5	0.03044	0.309972006	0.010766655	113.4298
	0.6	0.03041	0.178473013	0.006199132	96.20094
	0.3	0.03888	0.087283209	0.008364707	72.77678
60	0.5	0.1699	1.730730969	0.060115699	112.8925
	0.6	0.13926	0.817438314	0.028393134	97.33451
	0.3	0.0441	0.099087932	0.009496002	62.60502
90	0.5	0.1949	1.984248782	0.068921458	98.08689
	0.6	0.1599	0.938463598	0.03259686	85.9093

The simulation further combined 58 mm radius, 11 mm offset, and 0° twist and the optimal result was also recorded at TSR 0.5 as indicated by 3.046607 Watts power, 0.105822 Nm torque, and 0.29918 Power Coefficient (C_P) produced.

Table 6. Variations in Turbine Blade TSR

TSR	C_P	Power (Watt)	Torque (N.m)	Y Plus
0.3	0.06421	0.144118	0.013811	80.24362
0.5	0.29918	3.046607	0.105822	121.2431
0.6	0.25093	1.472946	0.051162	102.7176

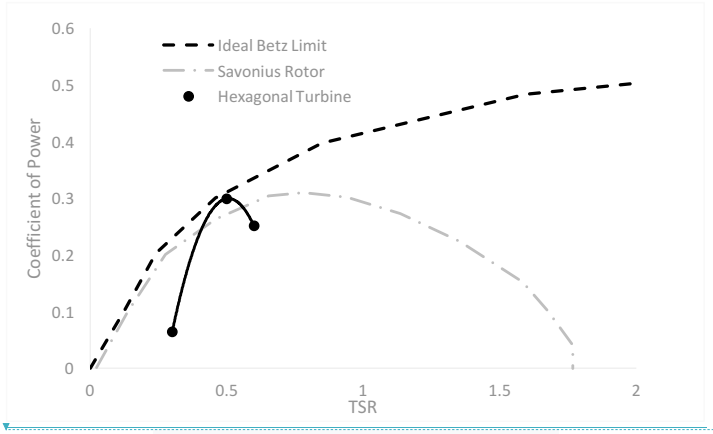

Figure18. Hexagonal Turbine Optimum Model

5. Conclusions

Deleted: From the results obtained, the

Deleted: is continued by trying to combine these three things, where is a radius of

Deleted: mm

Deleted: offset

Deleted: mm

Deleted: 0°

Deleted: value is

Deleted: with the power generated

Deleted: torque of 0.105822Nm. The

Deleted: value obtained is 0.29918

Deleted: Result of

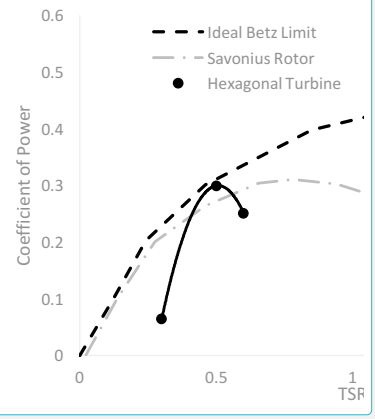

Deleted:

Numerical and CFD simulations were used to analyze the three parts of designing and optimizing the honeycomb module of Savonius micro wind turbine with 4 blades on the second façade building using radius, twist, and offset as the important factors to determine the performance.

The use of 58 mm radius, 11 mm offset, zero-degree twist blade, and 0.5 TSR in one-piece module design of the micro hexagonal wind turbine was found to have produced 3.047 watts of electricity which eliminated the piece modules of honeycomb photovoltaics (as explained in next research) while the optimal Power of Coefficient (C_p) was 0.29918.

The comparison of the Savonius turbine with the Hexagonal Turbine at a TSR of 0.5 showed the Hexagonal Turbine has a lower TSR leading to a smaller U_{inf} requirement. This prediction is associated with the 4 blades used in the design which is more than the Savonius turbine, thereby, causing an increment in the solidity which is very important for the VAWT more than the HAWT. It is also pertinent to note that the high solidity reduces the operating rotation of the wind turbine. Moreover, the Cp value of the Hexagonal Turbine was also found to be higher and close to the Betz limit which is the maximum allowed for wind turbines.

The previous design of Hexagonal Savonius with 4 blades at 90 mm radius as well as unknown offset and twist which was tested in wind tunnel produced only 0.03426 power of coefficient (C_p) and 0.12 watt of electricity. This, therefore, means the numerical and CFD simulation was successfully used to determine the optimal blade radius, offset, and twist to produce renewable energy in hexagonal micro wind turbine architectural building façade.

Deleted: The numerical …umerical and CFD simulati ... [41]

Deleted: With the blade radius …he use of 58 mm bla ... [42]

Deleted: When compared to …he comparison of the ... [43]

Deleted: Compared to …he previous design of Hexag ... [44]

References

Ahmed, M.M.A., Rahman, A.K.A., Ali, A.H.H., Suzuki, M. (2016). Double Skin Façade: The State of Art on Building Energy Efficiency. *Journal of Clean Energy and Technologies, 4(*1), 84-89.

Arteaga-López, E., Ángeles-Camacho, C., & Bañuelos-Ruedas, F. (2019). Advanced methodology for feasibility studies on building-mounted wind turbines installation in urban environment: Applying CFD analysis. *Energy*, *167*, 181–188. https://doi.org/10.1016/j.energy.2018.10.191

Attoye, D.E., Adekunle, T.O., Tabet Aoul, K., & Hassan, A., (2018). Building Integrated Photovoltaic (BIPV) Adoption: A Conceptual Communication Model for Research and Market Proposals. A Conference Proceeding ASEE Connecticut, USA.

Blackwell, B., Sheldahl, R., & Feltz, L. (1977). Wind Tunnel Performance Data for Two and Three Bucket Savonius Rotors. *Journal of Energy, 2*(3), 160-164.

Cao, X.D., Xilei, D., & Liu, J. (2016). Building Energy-Consumption Status Worldwide and the State-of-the-Art Technologies for Zero-Energy Buildings during the Past Decade. *Energy and Building*, *128*, 1-58.

California Energy Commission (2005). Options for Energy Efficiency in Existing Buildings.

Coyle, E.D., Grimson, W., Basu, B., Murphy, M. (2014). Understading the Global Energy Crisis. Book Chapter part 1: *Reflection on Energy, Greenhouses Gases, and Carbonaceous Fuels*. Purdue University Press.

Daryanto, Y. (2007). *Kajian Potensi Angin untuk Pembangkit Listrik Tenaga Bayu*. Yogjakarta: BALAI PPTAGG – UPT – LAGG.

Dudley, N. (2008). Climate Change and the Energy Crisis. Back to the Energy Crisis – the Need for a Coherent Policy towards Energy Systems. *Policy Matters*, *16*, 12-68.

Elger, D.F., LeBret, B.A., Crowe, C.T., & Robertson, J.A. (2015). *Engineering Fluid Mechanics* (9th ed.).

Ferrari, G., Federici, D., Schito, P., Inzoli, F., & Mereu, R. (2017). CFD Study of Savonius Wind Turbine: 3D model Validation and Parametric Analysis. *Journal of Renewable Energy, 105,* 722-734.

Howells, M., & Roehrl, R.A. (2012). Perspective on Sustainable Energy for the 21th Century (SD21). New York: United Nations Department of Economic Social Affairs, Division for Sustainable Development.

IEA. (2004b). Energy Balances for OECD Countries and Energy Balances for Non-OECD Countries, Energy Statistics for OECD Countries and Energy Statisics for Non-OECD Countries (2004 editions), Paris.

Kumar, A., & Saini, R.P. (2016). Performance Parameter of Savonius Type Hydrokinetic Turbine: A Review. *Journal of Renewable and Sustainable Energy Reviews*, *64*, 289-310.

Manienyen, V., Thambidurai, M., and Selvakumar, R. (2009). Study on Energy Crisis and the Future of Fossil Fuels. *Proceeding of SHEE, Engineering Wing, DDE*., Annamalai University, December 11-12, 2009.

Manwell, J.F., McGowan, J.G., & Rogers, A.L. (2010). *Wind Energy Explained: Theory, Design and Application* (2nd ed.). Wiley.

Mintorogo. D.S., Elsiana, F., & Budhiyantho, A. (2019). Experimental Sustainable Micro Wind Turbines on Second Façade of Buildings. A Research Report. Center for Research, Petra Christian University.

Nowak, D.J., Greenfield, E.J., & Ash, R.M. (2019). Annual Biomass Loss and Potential Value of Urban Tree Waste in the United States. *Urban Forestry & Urban Greening, 46*. 126469. https://www.fs.fed.us/nrs/pubs/jrnl/2019/nrs_2019_nowak_004.pdf. (June, 2020).

Park, J., Jung, H.J., Lee, S.W., Park, J. (2015). A new Building-Integrated Wind Turbine System Utilizing the Building. *Energies*, *8*, 11846–11870.

Rahman, M., Salyers, T.E., El-Shahat, A., Ilie, M., Ahmed, M., & Soloiu, V. (2018). Numerical and Experimental Investigation of Aerodynamic Performance of Vertical-Axis Wind Turbine Models with Various Blade Designs. *Journal of Power and Energy Engineering, 6*(5), 13-14. https://doi.org/10.4236/jpee.2018.65003

Suchde, P., Kuhnert, J., Schröder, S., & Klar, A. (2017). A flux conserving meshfree method for conservation laws. *International Journal for Numerical Methods in Engineering, 112*(3), 238–256. https://doi.org/10.1002/nme.5511

Sutrisno, Mirmanto, H., Sasongko, H., Noor, D. Z. (2015). Study of The Secondary Flow Structure Caused the Additional Forward-facing Step Turbulence Generator. *Advances and Applications in Fluid Mechanics* 18(1), 129-144.
http://dx.doi.org/10.17654/AAFMJul2015_129_144

Simanjuntak, M. E., Prabowo, Widodo, W. A., Sutrisno, Sitorus, M. B. H. (2019). Experimental and Numerical Study of Coal Swirls Fluidized Bed Drying on 10 ° Angle of Guide Vane. *Journal of Mechanical Science and Technology,* 33, 5499-5505.

Deleted: ;

Deleted: ;

Deleted: ;

Deleted: ;

https://doi.org/10.1007/s12206-019-1042-2.

Tahani, M., Babayan, N., Mehrnia, S., & Shadmehri, M. (2016). A Novel Heuristic Method for Optimization of Straight Blade Vertical Wind Turbine. *Energy Conversion and Management*, *127*, 461–476. https://doi.org/10.1016/j.enconman.2016.08.094

Wenehenubun, F., Saputra, A., & Sutanto, H. (2015). An experimental study on the performance of Savonius wind turbines related with the number of blades. *Energy Procedia*, *68*, 297–304. https://doi.org/10.1016/j.egypro.2015.03.259

Certificate of Proofreading

This document certifies that the manuscript was edited for proper English language, grammar, punctuation, spelling, and overall style by one or more of the highly qualified native English speaking editors at Good Lingua Center of Education (GLCE)

Manuscript Title

Harvesting Renewable Energies through Innovative Kinetic Honeycomb Facades: The Mathematical & CFD Modeling for Wind Turbine Design Optimization

Author(s)

Danny Santoso Mintorogo, Aris Budhiyanto, Feny Elsiana, Fandi D. Suprianto and Sutrisno

Date Issued

September 18, 2021

GoodLingua
Translation, editing, and proofreading

PT. Internasional Translasi Edukasi, Jakarta

2. Submitted to
“the Journal of Asian Architecture and Building Engineering” (9 -9-2021)

Submission Confirmation

Print

Thank you for your submission

Submitted to	Journal of Asian Architecture and Building Engineering
Manuscript ID	JAABE2211459EE
Title	The Implementation of architectural wind driven tubes roof-pond to save energy on roof cooling loads in tropical climate:CFD modeling and experimental investigations
Authors	Mintorogo, Danny Sutrisno, Sutrisno
Date Submitted	09-Nov-2022

Registration on Taylor & Francis Online

External

Inbox

Taylor & Francis <noreply@tandfonline.com> Nov 30, 2021, 9:18 AM

to me

e online platform for Taylor & Francis Online content

Dear Danny Mintorogo,

Thank you for registering an account at Taylor & Francis Online.

In order to complete the registration process we just need to confirm your email address.

Please click on the following link, or cut and paste the link into your web browser:

https://www.tandfonline.com/action/verifyEmail?activationCode=VuCdEztdCY2chRqDdShDxaUJ4g4zZD3r

Please note that this link is only valid for 14 days.

Once your account has been confirmed you will be able to purchase subscriptions, view paid content, and sign up to receive different alerts about titles and subjects you are interested in.

If you need help please visit the Taylor & Francis Online Help Centre.

Kind regards,
Taylor & Francis Online Customer Services

Please do not reply to this email. To ensure that you receive your alerts and information from Taylor & Francis Online, pleas "alerts@tandfonline.com" and "info@tandfonline.com" to your safe senders list.

Taylor & Francis, an Informa business.
Taylor & Francis is a trading name of Informa UK Limited, registered in England under no. 1072954. Registered office: 5 Howick Pl 1WG.

3. Received from Reviewers (01-9-2021)

Journal of Asian Architecture and Building Engineering - Decision on Manuscript ID JAABE2101027EE

External

Inbox

Journal of Asian Architecture and Building Engineering <onbehalfof@manuscriptcentral.com> Wed, Sep 1, 2021, 8:50 AM

to me, lxlst

01-Sep-2021

Dear Dr. Mintorogo,

Manuscript ID JAABE2101027EE entitled "Harvesting Renewable Energies by Innovative Kinetic Honeycomb Facades: Mathematical & CFD Modeling for Optimizing Wind Turbine Design" which you submitted to the Journal of Asian Architecture and Building Engineering, was determined to need further revision to be accepted for the publication.

The review comments are included at the bottom of this letter.
Please respond to the comments and revise your manuscript.

To revise your manuscript, log into https://mc.manuscriptcentral.com/jaabe and enter your Author Dashboard, where you will find your manuscript title listed in "Manuscripts with Decisions." Click on "Create a Revision." Your manuscript number has been appended to denote a revision.

Because we are trying to facilitate timely publication of manuscripts submitted to the Journal of Asian Architecture and Building Engineering, your revised manuscript should be uploaded within FOUR WEEKS.

You will be unable to make your revisions on the originally submitted version of the manuscript. Instead, revise your manuscript using a word processing program and save it on your computer. Please also highlight the changes to your manuscript within the document by using the track changes mode in MS Word or by using colored text (red text).

Once the revised manuscript is prepared, you can upload it and submit it through your Author Center.

When submitting your revised manuscript, you will be able to respond to the comments made by the reviewer(s) in the space provided. You can use this space to document any changes you make to the original manuscript. In order to expedite the processing of the revised manuscript, please be as specific as possible in your response to the reviewer(s).

IMPORTANT: Your original files are available to you when you upload your revised

manuscript. Please delete any redundant files before completing the submission.

Once again, thank you for submitting your manuscript to the Journal of Asian Architecture and Building Engineering and I look forward to receiving your revision.

IMPORTANT INFORMATION

Authors (first author and co-authors)* shall not be changed after initial manuscript submission. *The addition and deletion of authors are unacceptable. *The order of authors can not be changed.

If manuscript is required the native language check in the review comments, please be sure to upload and submit the following with your revised manuscript files:

[PDF] English Proof Certificate (issued by English editing company) *The charges should be owned by authors.

Please contact to the Secretarial Office (TABE-peerreview@journals.tandf.co.uk), if you have any questions.

Sincerely,

Prof. Moonseo Park
Associate Editor, Journal of Asian Architecture and Building Engineering

Editor(s)' Comments to Author:

Field Editor: 1
Comments to the Author:
(There are no comments.)

Field Editor: 2
Comments to Author::
(There are no comments.)

Reviewer(s)' Comments to Author:

Reviewer: 1

Comments to be returned to author(s)
1. The research quoted in the abstract is confusing since it is inconsistent with the title. Are they refer to the same topic?
2. The abstract contains inappropriate use of capital letters for sentence: “THE WORLD in the field of ARCHITECTURE in multilevel buildings now could harvest sustainable greenery energies in a smart façade”.
3. The redundant words are used here: “The idea was taking a honeycomb form

(bio-mimicry) in the hexagonal (hexagonal) shape of facets…"
4. The acronym BIPV should be introduced in the first time it appears.
5. The acronym BIWT should be introduced in the first time it appears.
6. Inappropriate bold letters are used in the text: "Horizontal Rotor (windmills with a vertical rotating shaft and horizontal rotor) and Vertical Rotor (an upright player with a horizontal propeller rotation)"
7. Reference is needed here: "Based on the previous experimental design of Savonius type of wind turbine with 4 blades, the experimental model was tested in the wind tunnel at Mechanical Engineering laboratory, with the result of Cp of only 0.003426."
8. Figure 6 is not clear. The geometry is better presented in white background.
9. The word "Torsi" in Table 2-5 is not a correct English term.
10. The sentence has redundant components: "Figure 9 shows that the three models (radius 58, 64, and 72) that had the highest CP values had the same flow velocity patterns that were closely similar".
11. Reference is needed here: Figure 15 (A)
12. Figure 15 should be put in the Result and Discussion section, instead of Conclusion.
13. The authors refer to the previous works with both numerical and experimental data but failed to present the result or provide a reference for it. It is important to present validation of the numerical simulation either from the authors' own data or appropriate reference. Further analysis on the simulation's result validity should also be presented.

4. Revised manuscripts with special note (21-9-2021)

Comment notes based on reviewer 1 have been revised. (the corrections are in the paper MS Word).

1. The research quoted in the abstract is confusing since it is inconsistent with the title. Are they refer to the same topic?
Yes, it is the same topic but different expression words. I forgot to change the title in the abstract. I Have revised it. → [The research, harvesting renewable energies by innovative kinetic honeycomb architectural facades with micro wind turbine].

2. The abstract contains inappropriate use of capital letters for sentence: "THE WORLD in the field of ARCHITECTURE in multilevel buildings now could harvest sustainable greenery energies in a smart façade".
On page 1. I have revised the words in the sentence. → [The architecture domain in multilevel buildings now can harvest sustainable greenery energies].

3. The redundant words are used here: "The idea was taking a honeycomb form (bio-mimicry) in the hexagonal (hexagonal) shape of facets…"
On page 3. Yes, it is redundant words. I revised it (section 2.1).-->[thousands of hexagonal ~~honeycomb~~ micro-module wind turbines].

4. The acronym BIPV should be introduced in the first time it appears.
On page 4. It was added to the introduction section and section 2.1 → [The term BIPV (Building Integrated Photovoltaic)].

5. The acronym BIWT should be introduced in the first time it appears.
On page 4. It was added to section 2.1 & figure 6. → [Building Integrated Wind Turbine (BIWT)].

6. Inappropriate bold letters are used in the text: "Horizontal Rotor (windmills with a vertical rotating shaft and horizontal rotor) and Vertical Rotor (an upright player with a horizontal propeller rotation)"
on page 5. It was revised all. → [the location of the horizontal rotor ~~(Horizontal Rotor)~~ and an upright player]

7. Reference is needed here: "Based on the previous experimental design of Savonius type of wind turbine with 4 blades, the experimental model was tested in the wind tunnel at Mechanical Engineering laboratory, with the result of Cp of only 0.003426."
on page 5. It has been added reference (section 3). → [Whereas at a wind speed of 5 m/s, it produced 3.39 Volts. and 0.01 Amperes. Power 0.0607 Watt. (Mintorogo, 2019).].

8. Figure 6 is not clear. The geometry is better presented in white background.
On page 5. Figure 6 has been redrawn.

9. The word "Torsi" in Table 2-5 is not a correct English term.
Table 3 to 6. It revised. → [Torque (N.m)].

10. The sentence has redundant components: "Figure 9 shows that the three models (radius 58, 64, and 72) that had the highest CP values had the same flow velocity patterns that were closely similar".

On page 11. It has delated the redundant words. → [The picture 12 can be seen that the three models (radius 58, 64 and 72) that have the highest C_P values have the same flow velocity patterns.].

11. Reference is needed here: Figure 15 (A)
On page 13. It was added a reference.

12. Figure 15 should be put in the Result and Discussion section, instead of Conclusion.
On page 5. It was put into figure 7.

13. The authors refer to the previous works with both numerical and experimental data but failed to present the result or provide a reference for it. It is important to present validation of the numerical simulation either from the authors' own data or appropriate reference. Further analysis on the simulation's result validity should also be presented.
On page 8 – 10. The Simulation Validation data is showed on section 3.3

3.3 Simulation Validation

The validation process was conducted using a 3D model in accordance with Ferrari et al. and this involved the Savonius turbine model being in line with the Rotor C geometry [Ferrari, 2017]. Moreover, the Reynolds number used was based on turbine diameter (Dt) and bulk velocity (U_{inf}) which was 4.32 .105 while the wind tunnel was in line with the method applied by Blackwell et al., and the 1.4% Turbulence Intensity used was in accordance with 1% recommended by Suchde et al. (2017, 255). The two simulations conducted with the experimental results of Blackwell et. al. 1977 in the wind tunnel showed that the most optimal Savonius turbine was found at approximately TSR 0.85 with a maximum Coefficient of power (Cp) value of 0.25 as indicated in Figure 9. The other TSR variables used based on the angular velocity of the rotor turbine include 0.576, 0.804, and 1.002 while the coefficient of power value was used for comparison. Moreover, the experimental trend of the Savonius turbine performance was presented through the simulation conducted using Ansys Fluent 16.0 with 3D Dimensional, Double Precision, Pressure-Based Solver, Steady-State Condition, and Criteria Convergency 10-5. The Cell Zone conditions were also divided into static and dynamic frames with the dynamic conditions specifically having the frames of motion with rotational velocity.

The simulation results of hexagonal micro wind turbine were compared with the Ferrari et al. findings and this study was discovered to have a smaller Cp due to its use of a mathematical model approach which led to some flow phenomena such as the turbulent flow which was observed to have been developing continually up to the present moment. Sutrisno et al. (2015) reported turbulence intensity as an energy reserve being converted gradually to flow and this means the flow with high turbulence tends to have stronger energy. Meanwhile, another flow phenomenon known as the swirl flow was reported by Simanjuntak et al. (2019) to have the capability to be used as a major factor in the coal drying process due to its ability to separate steam vapor in soil coal. The Savonius turbine simulation, however, used very strong turbulence and swirl flow phenomena, thereby, causing high uncertainty.

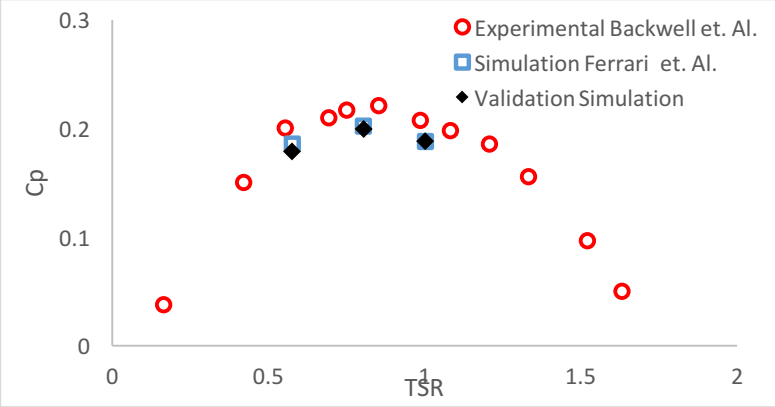

Figure 9. Comparison between the simulation results of Hexagonal micro wind turbine to Ferrari et al. and Blackwell et al.

The validation results of hexagonal micro wind turbine showed large error values of 10.45%, 10.02%, and 9.43% at TSR 0.576, 0.804, 1.002 respectively as presented in Table 2. This means the model was unable to produce better predictions than Ferrari et al.'s prediction of the experimental results of Blackwell et al due to its use of a steady-state condition. It was, therefore, recommended that the unsteady state simulation approach which requires resource computation with high-performance equipment be used in further studies. Meanwhile, some other parameters were selected for the next process which involved optimizing the hexagonal turbine design. This validation method only compares one parameter due to the focus of this study on the optimization of a new design for the Savonius turbine shape.

Table 2. Comparison of the simulation validation result with the experiment of the Blackwell et al. (1977).

TSR	Simulation Validation	Error % Cp with Experiment Blackwell et al.
0.576	0.1791	10.45
0.804	0.1994	10.02
1.002	0.1883	9.43

On page 16. The conclusion was rewritten.

Numerical and CFD simulations were used to analyze the three parts of designing and optimizing the honeycomb module of Savonius micro wind turbine with 4 blades on the second façade building using radius, twist, and offset as the important factors to determine the performance.

The use of 58 mm radius, 11 mm offset, zero-degree twist blade, and 0.5 TSR in one-piece module design of the micro hexagonal wind turbine was found to have produced 3.047 watts of electricity which eliminated the piece modules of honeycomb photovoltaics (as explained in next research) while the optimal Power of Coefficient (C_p) was 0.29918.

The comparison of the Savonius turbine with the Hexagonal Turbine at a TSR of 0.5 showed the Hexagonal Turbine has a lower TSR leading to a smaller U_{inf} requirement. This prediction is associated with the 4 blades used in the design which is more than the Savonius turbine, thereby, causing an increment in the solidity which is very important for the VAWT more than the HAWT. It is also pertinent to note that the high solidity reduces the operating rotation of the wind turbine. Moreover, the

Cp value of the Hexagonal Turbine was also found to be higher and close to the Betz limit which is the maximum allowed for wind turbines.

The previous design of Hexagonal Savonius with 4 blades at 90 mm radius as well as unknown offset and twist which was tested in wind tunnel produced only 0.03426 power of coefficient (C_p) and 0.12 watt of electricity. This, therefore, means the numerical and CFD simulation was successfully used to determine the optimal blade radius, offset, and twist to produce renewable energy in hexagonal micro wind turbine architectural building façade.

5. Revised manuscripts with highlights (21-9-2021)

Harvesting Renewable Energies through Innovative Kinetic Honeycomb Architectural Facades: The Mathematical & CFD Modeling for Wind Turbine Design Optimization

Danny Santoso Mintorogo[1*], Aris Budhiyanto[1], Feny Elsiana[1], Fandi D. Suprianto[2], & Sutrisno[2]
[1]Department of Architecture, Petra Christian University
[2]Department of Mechanical Engineering, Petra Christian University
Siwalankerto street no. 121-131, East-Java, Indonesia
[*]Corresponding author; Email: dannysm@petra.ac.id

Abstract
The research was conducted on harvesting renewable energies through innovative kinetic honeycomb architectural facades using micro-wind turbines, photovoltaics, and natural light pipes in buildings. It was specifically focused on the renewable energy factors associated with thousands of hexagonal micro-module wind turbines, hexagonal solar cell modules, and hexagonal modules for solar-reflecting pipes usually applied for deep sunlight reflection into a room of a building which has a veiled facade on the outside. This involved the utilization of windmills and solar cells specifically designed in a non-structural facade of the front building envelope through a double facade technique. Moreover, electrical energy was obtained from each windmill module while extra renewable electricity from abundant sunlight was acquired through the hexagonal modules of the solar cells (photovoltaic) designed vertically on the building facade. This means this current research only focuses on hexagonal wind turbines. Furthermore, ANSYS Fluent 12.0 simulated software and numerical analysis were used to optimize and redesign the wind turbine blades in order to obtain more electricity from one micro-module hexagonal wind turbine. The results showed that this design was able to produce 2.66 Watts per wind turbine compared to the 0.12 Watt from the previous design. The TSR was also found to be 0.5 and its power coefficient value (C_P) of 0.4525 was observed to be much higher than the 0.0343 from the previous design. This, therefore, means the architecture domain in multilevel buildings has the ability to harvest sustainable greenery energies from such a smart architectural façade.

Keywords: Harvest renewable energy, kinetic honeycomb architectural façade, numerical and simulated CFD, wind turbines design for second façade architecture buildings.

1. Introduction

The world has been experiencing an extreme global energy crisis since 1979 due to the high need for energy (Manieniyen, 2009). Several countries have, therefore, been exploiting conservative biomass such as fossil fuels in the form of gasoline, coal, oil, propane, and natural gas. According to the United States Energy Information Administration (EIA), un-canopies natural energies are usually used and these include 80% from fossil fuels as indicated by 35,3% petroleum, 19,6% coal, and 26,6% natural gas while only 8,3% is from nuclear energy, and 9.1% from renewable energy (Coyle, 2014, p.15). Moreover, nuclear reactors currently use uranium (U), plutonium (Pu), and thorium (Th) as fuel to produce energy. This led to the search for eco-friendly environmental energies from hydrogen as the alternative gasoline in order to reduce CO2 pollution and asthma prevalence. There are other eco-friendly energy sources except hydro-energy and nuclear power and these include solar power or photovoltaics which involves using the abundant sun rays through solar radiation to generate electricity. The process involves installing either fixed or rotatable solar panels for approximately 10 hours on rooftops, canopies, or facades. Another alternative is the force-moving kinetic wind or wind turbines which generate electricity silently for almost 24 hours (Dudley, 2008, p.39). Biomass is another option through direct heating or biomass boilers and involves burning urban dry leaves or pruned trees as well as house and farm unused papers to generate energy while increasing household incomes and reducing city garbage (Nowak et al., 2019).

Renewable energies are becoming more important in cities and rural areas due to the high demand for energy in recent decades for residential and commercial purposes, especially in remote areas such as islands located very far from government power plants (Daryanto, 2007). Previous studies showed that 31% of energy is consumed through transportation while residential and commercial buildings use nearly 40%-42% (Cao, Xilei & Liu, 2016) and have the greatest total essential energy consumed in the U.S. and E.U (EIA, 2004b). Moreover, the Energy Efficiency Division of the Philippines Department of Energy (DOE) (2002) showed that 15 to 20% of the total national energy in the country was consumed by buildings and industries while a higher percentage of 66% was reported in California, USA (California Energy Commission, 2005). It was also predicted that the energy needed by this sector from different sources in countries which are not members of the Organization for Economic Cooperation and Development Countries (OECD) between 2010 to 2050 is expected to increase from 50 quadrillions BTU to approximately 32 - 82 quadrillion BTU while the value required by OECD members is expected to be from 7 quadrillions BTU to approximately 48 to 55 quadrillion BTU as indicated in Figure 1.

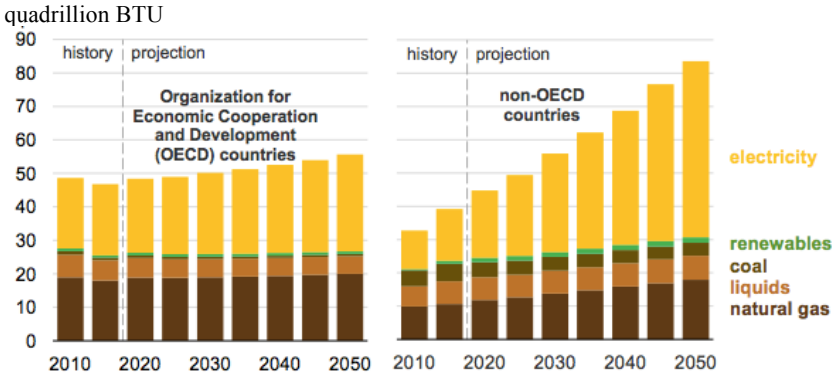

Source: U.S. Energy Information Administration. *International Energy Outlook 2019*

Figure 1. Energy Consumption in Buildings by Many Energy Resources (2010-2050)

This means more renewable energy is needed to generate and harvest sustainable electricity for residential and commercial or rental office buildings considering the small quantity it presently contributes when compared to the normal fossil oil as indicated in Figure 1. Countries of the world are observed to be constructing and consuming renewable energy, especially from solar and wind sources, as indicated by the annual average increase of 3.6% from 2018 to 2050 and a gradual decrease in coal-based energy consumption from 35% in 2018 to 22% at the end of 2050. This means coal is the current primary source while renewable energy is projected to contribute 50% of the total world electricity production in 2050 (International Energy Outlook, 2019). It is also important to note that Building Integrated Photovoltaics System (BIPV) through thousands of solar cells has also been installed across the world from 2013 to 2019 to generate around 5.4 GW and annual growth of 18.7% (Attoye, 2018).

The objective of this research was to propose and obtain renewable energies on building facades using honeycomb module wind turbines.

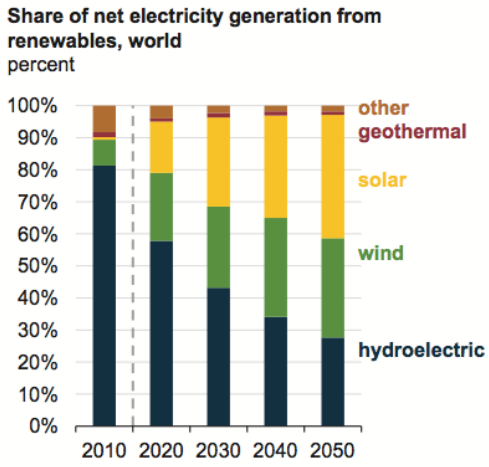

Source: U.S. Energy Information Administration. *International Energy Outlook 2019*

Figure 2. World Net Electricity Production from Renewable Sources (2010-2050)

2. Renewable Energy

The focus of this research is on renewable energy from solar and wind sources using a smart energy honeycomb façade. This façade depends on a double skin façade which has three parts which include the upper-part hexagonal module in the form of series of horizontal light pipes built on room ceilings to tap energy from daylight. The middle-part honeycomb module façades consist of thousands of micro-wind turbines to tap energy from kinetic wind sources while the bottom-part hexagonal modules include thousands of photovoltaic cells used to harness energy from solar radiation as indicated in Figures 3A and B.

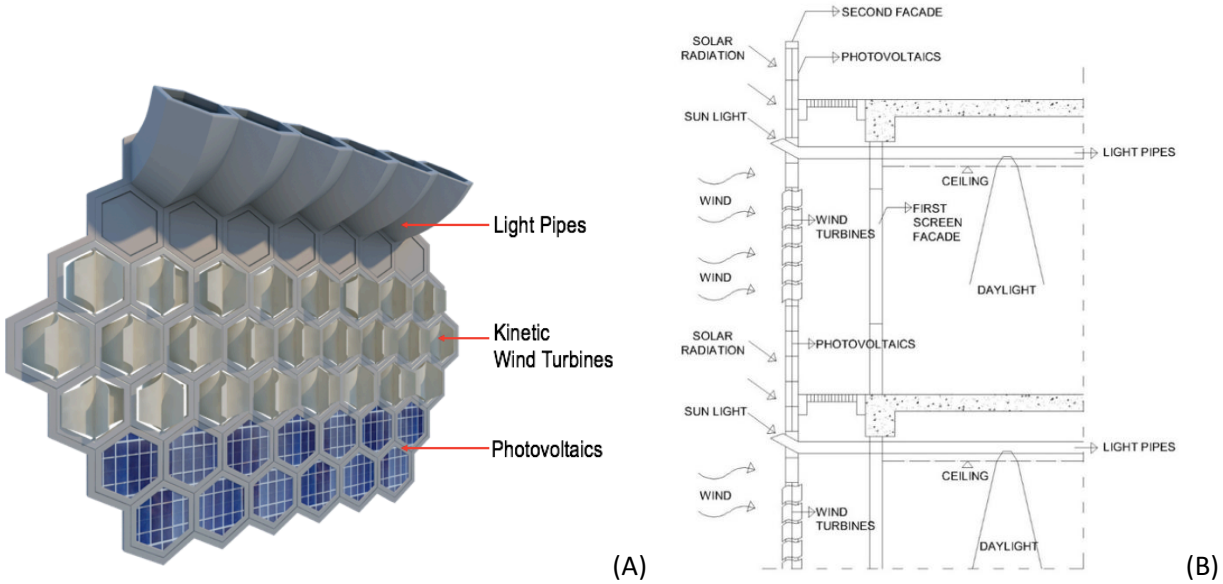

. (A) (B)

Figure 3. (A) Conceptual Double Skin Smart Façade (Light-Pipes, Wind Turbines, Photovoltaic Cells). (B) Schematic Building Section-Drawing showing features of light pipes, wind turbines, and photovoltaics.

2.1. Biomimicry Smart Façade Concept

The common double facade building technique applied has been reported to be very effective for energy conservation for a long period (Ahmed, 2016). It is also designed to save energy and assist in the process of collecting renewable energies as a contribution to finding solutions to the world energy crisis.

Moreover, the idea of using the honeycomb form or bio-mimicry was based on the (1) regular modular to represent the rigidity of the facade structure and 2) each hexagon module is filled with honey which serves as the source of life for children of bees known as larvae and the queen bees as indicated in Figure 4A. This design is projected to retrieve renewable electricity using thousands of small windmills placed in one-third of the smart facade as shown in Figure 4B while solar cells are on the lower part and the hexagon-shaped reflection pipes are at the top as indicated in Figure 3A.

(A)

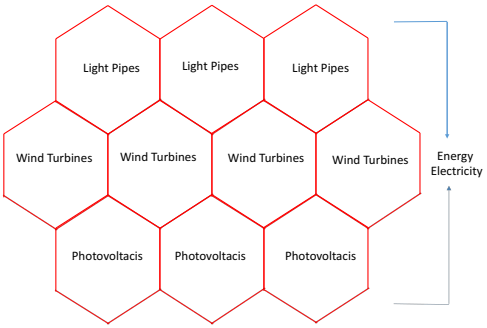

(B)

Figure 4. (A) Honeycomb, bees, and honey and (B) Honeycomb smart façade module and electricity

The term BIPV (Building Integrated Photovoltaic) is normally used to define buildings incorporated with PV circuits on the roof or envelope system. IBIPV systems can be used to replace roofing, curtain walls, glazing, or special elements such as eaves or canopies. It is usually applied in the concept of green architecture as an energy-saving strategy through the utilization of solar radiation which is an environmentally friendly renewable energy source (Howells & Roehrl, 2012). Meanwhile, Building Integrated Wind Turbine (BIWT) is a building designed using wind turbines in the facades to produce energy (Arteaga-López, Ángeles-Camacho, & Bañuelos-Ruedas, 2019).

2.2. Renewable Wind Turbines Energy Systems

An example of renewable energy from wind is the windmill which can be divided into horizontal and vertical types. These two types have the same mechanism and this involves the wind moving the propeller which later drives the motor to produce electrical energy but the difference is observed from the placement of the quite heavy motor. It is, however, important to note that the vertical type is more advantageous due to its ability to match the weight of gravity which is straight down. Moreover, the movement of the propeller on the wind turbine due to kinetic energy as the wind pushes its surface depends on its horizontal or vertical placement. This classification was also observed in the rotation of the shaft as indicated by the one rotating vertically when the rotor is located in a horizontal position as well as the horizontal rotation when the rotor was placed vertically which has been further developed into Savonius, Darrieus, and H-Rotor as indicated in Figure 5A.

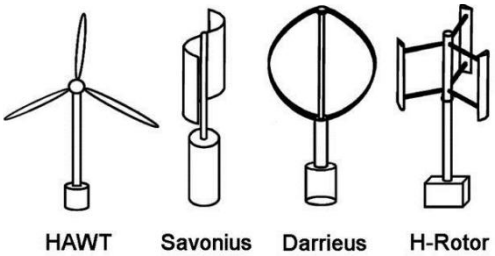

(A)

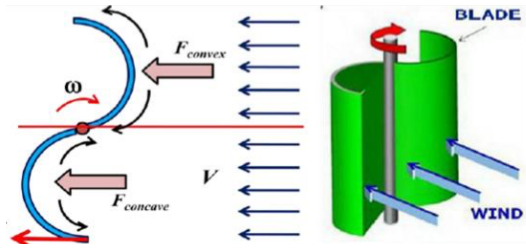

(B)

Figure 5. Horizontal and Vertical Rotating Propeller Placement (A) Principles of Wind Turbine Movement in the Savonius System (B)

The wind turbine spins due to the difference in pressure on each blade. For example, one of the sunken sides of the Savonius vertical wind turbine captures the wind and spins it while the other side of the convex receives also wind and causes the turbine to spin as shown in Figure 5B (Wenehenubun, Saputra, & Sutanto, 2015). It is possible to turn the wind turbines in tall buildings over using two systems. The first involves using several large wind turbines placed on the roof of a building, between two adjacent buildings, or in a hole created inside the building as indicated in Figure 6A and this design can be found in the World Trade Center building in Bahrain. The second method is using many small wind turbines installed on buildings as showed in Figure 6B and this is considered advantageous due to the fact that the size of the turbines reduces its ability to overload the building structure but requires to be installed in high number to produce the energy needed. An example of these designs can be found in the Miami Coral Tower in Miami (Park, Jung, Lee, & Park, 2015). Meanwhile, Savonius VAWT (S-VAWT) is a good candidate due to its high initial torque, low cost, easy installation and repair, and sturdiness (Manwell et al., 2010, 1-3).

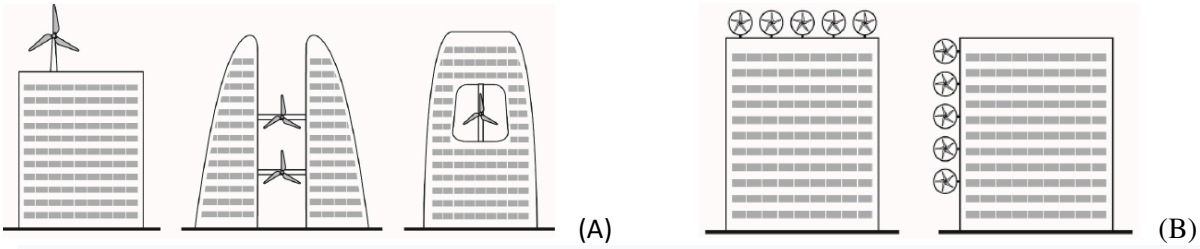

Figure 6. (A) Three Building Integrated Wind Turbine (BIWT) Systems using Large Wind Turbines and (B) Two BIWT Systems Use Small Sized Wind Turbines. (Source: Park, 2015).

3. Methodology Overview

The purpose of this research was to obtain the maximal values of electrical power from wind turbines' hexagonal frame smart façade module. It was focused on redesigning the wind turbine blades numerically after which they were simulated using ANSYS Fluent which is a simulation computational fluid dynamic (CFD) analysis program.

The previous experimental design of the Savonius wind turbine with 4 blades was used as the basis for the experimental model tested in the wind tunnel at the Mechanical Engineering laboratory and the Cp was found to be only 0.003426. Meanwhile, one module of hexagonal windmill produced 2.30 Volts, 0.05 Ampere, and 0.1182 Watt when the wind speed was 4 m/s while the values were 3.39 Volts, 0.01 Amperes, and 0.0607 Watt at 5 m/s (Mintorogo, 2019).

3.1. Shape and Size of Integrated Windmills in the Building Façade

The facade in the building has a small windmill dimension known as a micro wind turbine with the longest diameter being 0.30 meters while the shortest was 0.25981 meters. Moreover, the total area of the hexagons was 0.0585 m2 as indicated in Figure 7A. The "Savonius" Windmill was selected based on the consideration that it is the simplest method and works based on the differences in shear force or differential drag windmill as shown in Figures 7B and C.

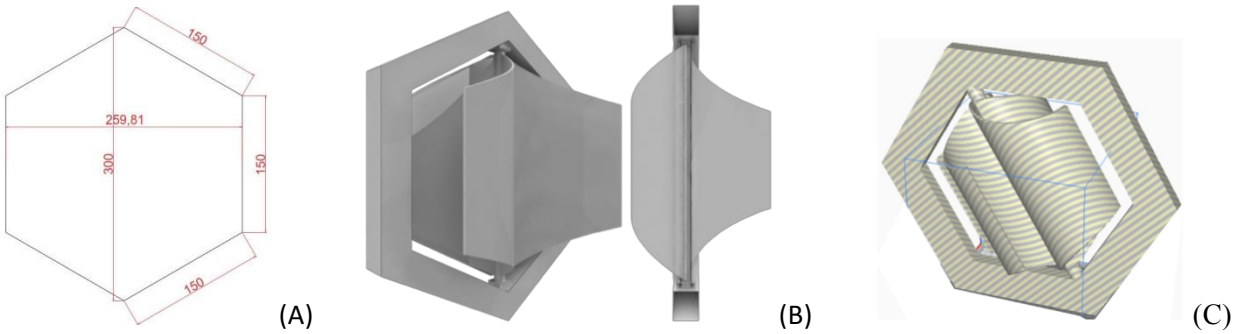

Figure 7. (A) Dimension of Honeycomb Windmill module,
(B) Previous Design of Savonius Wind Turbine model, and (C) Optimized Savonius Wind Turbine Module with 4 Blades

3.2. Basic Theory for the Wind Turbine

Turbines are devices used in converting kinetic energy from the wind into motion energy. The amount of energy or turbine power (P) can theoretically be written as follows:

$$\mathrm{P} = \mathrm{T}\omega \tag{1}$$

Where:
P = Turbine power $(watt)$.
T = Torque or moment of the turbine (Nm).
ω = Angular velocity of the turbine (*rad/s*).

The area passed by the air was designed to have the same boundary end to the end and used as a reference value in the ANSYS Fluent 12.0 to determine the moment coefficient. Meanwhile, the dimensionless moment coefficient in line with Rahman et al. (2018, 13) is, therefore, stated as follows:

$$C_m = \frac{T}{\frac{1}{4}\rho A D V^2} \tag{2}$$

Where:
C_m = Moment coefficient.
ρ = Fluid density (kg/m^3).
A = Turbine blade cross-sectional area (m^2).
D = Diameter of the turbine (m).
V = Fluid velocity (m/s).

The aerodynamics in turbines also consist of several forces known as dimensionless forces such as the density and speed of the freestream body. The relationship between these two values is, however, expressed as dynamic pressure and represented using the following equation.

$$q_\infty = \frac{1}{2}\rho_\infty {V_\infty}^2 \tag{3}$$

This means it is possible to define the dimensionless force as follows:
Lift coefficient: $C_L = \frac{L}{q_\infty S}$
Drag coefficient: $C_D = \frac{D}{q_\infty S}$
Normal force coefficient: $C_N = \frac{N}{q_\infty S}$
Axial force coefficient: $C_A = \frac{A}{q_\infty S}$
Where:
L = Lifting force (N)
D = Drag force (N)
N = Normal force (N)
A = Axial force (N)
S = Extensive reference area (m^2)

The S or reference area in the coefficient was selected based on the shape of the body geometry and the values for different shapes are presented in Table 1.

Table 1. Cd values for different body shapes

Type of Body	Length Ratio	Re	C_D
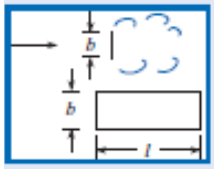 Rectangular plate	$l/b = 1$	$>10^4$	1.18
	$l/b = 5$	$>10^4$	1.20
	$l/b = 10$	$>10^4$	1.30
	$l/b = 20$	$>10^4$	1.50
	$l/b = \infty$	$>10^4$	1.98
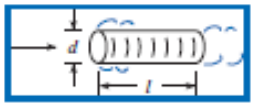 Circular cylinder with axis parallel to flow	$l/d = 0$ (disk)	$>10^4$	1.17
	$l/d = 0.5$	$>10^4$	1.15
	$l/d = 1$	$>10^4$	0.90
	$l/d = 2$	$>10^4$	0.85
	$l/d = 4$	$>10^4$	0.87
	$l/d = 8$	$>10^4$	0.99
Square rod	∞	$>10^4$	2.00
Square rod	∞	$>10^4$	1.50
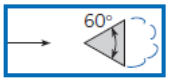 Triangular cylinder	∞	$>10^4$	1.39
Semicircular shell	∞	$>10^4$	1.20
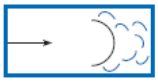 Semicircular shell	∞	$>10^4$	2.30
Hemispherical shell		$>10^4$	0.39
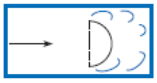 Hemispherical shell		$>10^4$	1.40
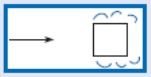 Cube		$>10^4$	1.10
Cube		$>10^4$	0.81
Cone—60° vertex		$>10^4$	0.49
Parachute		$\approx 3 \times 10^7$	1.20

(Source: Elger et al., 2015, 371–372)

It is possible to capture some of the kinetic energy passing through the turbine cross-section and this is expressed as the power coefficient (Cp) which can be calculated using the following formula:

$$C_p = \frac{P}{\frac{1}{2}\rho ADV^3} = \frac{T\omega}{\frac{1}{2}\rho ADV^3} = \lambda C_m \quad (4)$$

Where:
C_p = power coefficient
P = power of the turbine (Watt).

The power coefficient of this turbine, however, depends on the Tip-Speed Ratio (TSR) which is the ratio of blade speed at the tip to the speed of airflow as indicated in the following relationship:

$$\lambda = \frac{\omega R}{V} \quad (5)$$

Where:
λ = Tip-speed ratio
R = Turbin radius (m)

The theoretical power coefficient limit is 0.59 and this is known as the Betz Limit. Meanwhile, Figure 8 shows the maximum value of the power coefficient (C_p) against TSR for different types of turbines (Kumar & Saini, 2016, 293)

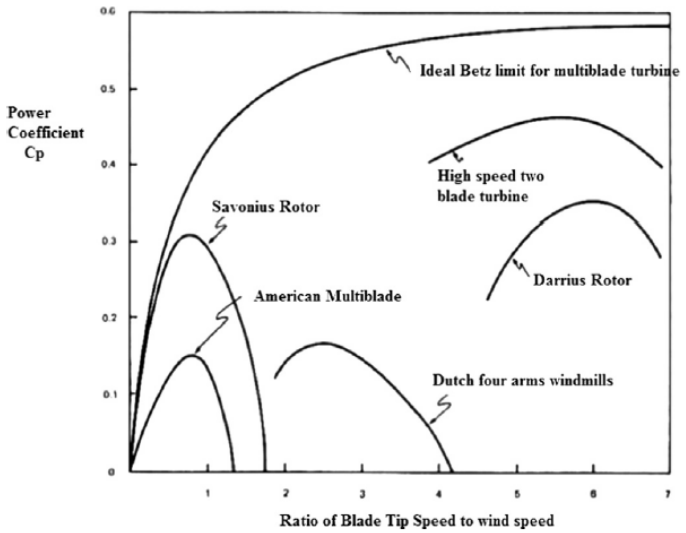

Figure 8. Power Coefficient against TSR

3.3. Simulation Validation

The validation process was conducted using a 3D model in accordance with Ferrari et al. and this involved the Savonius turbine model being in line with the Rotor C geometry [Ferrari, 2017]. Moreover, the Reynolds number used was based on turbine diameter (Dt) and bulk velocity (U_{inf}) which was 4.32 .105 while the wind tunnel was in line with the method applied by Blackwell et al., and the 1.4% Turbulence Intensity used was in accordance with 1% recommended by Suchde et al. (2017, 255). The two simulations conducted with the experimental results of Blackwell et. al. 1977 in the wind tunnel showed that the most optimal Savonius turbine was found at approximately TSR 0.85 with a maximum Coefficient of power (Cp)

value of 0.25 as indicated in Figure 9. The other TSR variables used based on the angular velocity of the rotor turbine include 0.576, 0.804, and 1.002 while the coefficient of power value was used for comparison. Moreover, the experimental trend of the Savonius turbine performance was presented through the simulation conducted using Ansys Fluent 16.0 with 3D Dimensional, Double Precision, Pressure-Based Solver, Steady-State Condition, and Criteria Convergency 10-5. The Cell Zone conditions were also divided into static and dynamic frames with the dynamic conditions specifically having the frames of motion with rotational velocity.

The simulation results of hexagonal micro wind turbine were compared with the Ferrari et al. findings and this study was discovered to have a smaller Cp due to its use of a mathematical model approach which led to some flow phenomena such as the turbulent flow which was observed to have been developing continually up to the present moment. Sutrisno et al. (2015) reported turbulence intensity as an energy reserve being converted gradually to flow and this means the flow with high turbulence tends to have stronger energy. Meanwhile, another flow phenomenon known as the swirl flow was reported by Simanjuntak et al. (2019) to have the capability to be used as a major factor in the coal drying process due to its ability to separate steam vapor in soil coal. The Savonius turbine simulation, however, used very strong turbulence and swirl flow phenomena, thereby, causing high uncertainty.

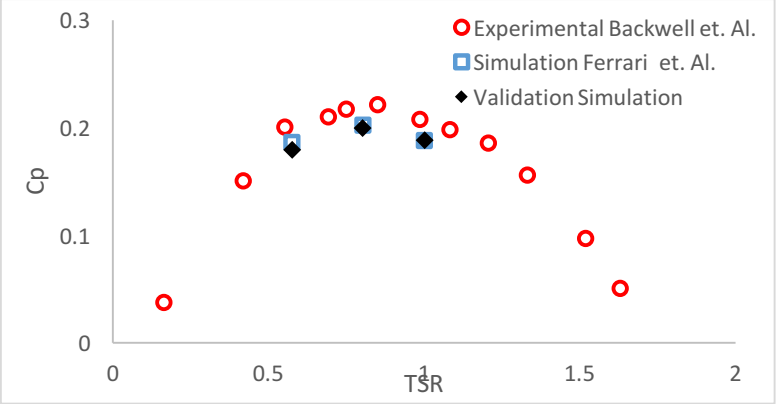

Figure 9. Comparison between the simulation results of Hexagonal micro wind turbine to Ferrari et al. and Blackwell et al.

The validation results of hexagonal micro wind turbine showed large error values of 10.45%, 10.02%, and 9.43% at TSR 0.576, 0.804, 1.002 respectively as presented in Table 2. This means the model was unable to produce better predictions than Ferrari et al.'s prediction of the experimental results of Blackwell et al due to its use of a steady-state condition. It was, therefore, recommended that the unsteady state simulation approach which requires resource computation with high-performance equipment be used in further studies. Meanwhile, some other parameters were selected for the next process which involved optimizing the hexagonal turbine design. This validation method only compares one parameter due to the focus of this study on the optimization of a new design for the Savonius turbine shape.

Table 2. Comparison of the simulation validation result with the experiment of the Blackwell et al. (1977).

TSR	Simulation Validation	Error % Cp with Experiment Blackwell et al.
0.576	0.1791	10.45
0.804	0.1994	10.02

1.002	0.1883	9.43

4. RESULTS and DISCUSSION

The software used for simulation was ANSYS FLUENT 16.0 using the following parameters:
Viscous model: RNG k-epsilon, Standard Wall Function.
Rotational velocity: varied to obtain a different TSR
Velocity inlet : 4 m/s
Turbulent method: Intensity and length scale
Turbulent length scale: 0.001 m
Turbulent intensity : 5 % depend on wind tunnel
3D model & meshing: gambit software

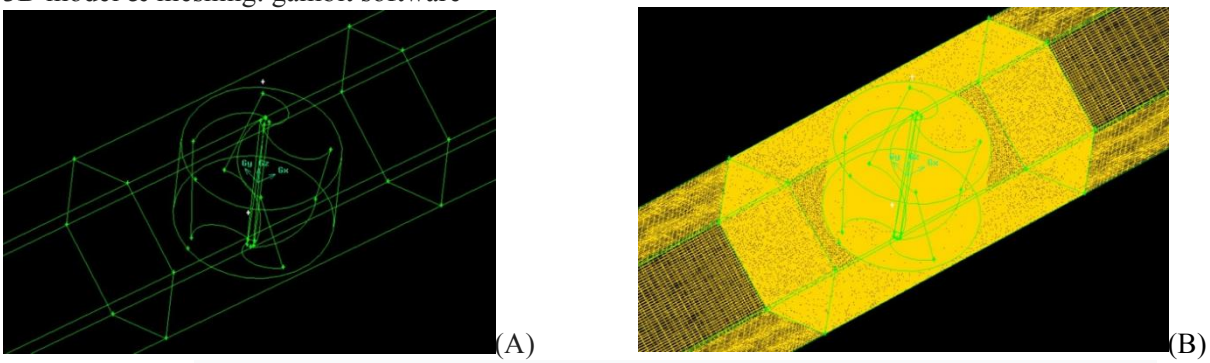

(A) (B)

Figure 10. (A) Savonius 3D facet 3D model and (B) Savonius 3D meshing model

There is a variation in the radius, offset, and twist of the hexagonal or honeycomb wind turbine blades used. The simulation was conducted to obtain the value of the Power Coefficient for the Savonius hexagonal wind turbine using 6 radii which include 57.5 mm, 58 mm, 60 mm, 64 mm, 72 mm, and 87.4 mm as showed in Figure 11A, 5 offsets including 0 mm, 5 mm, 7 mm, 9 mm, and 11 mm as indicated in Figure 11B, and the 5 twist models including 0^o, 30^o, 45^o, 60^o, and 90^o as presented in Figure 11C. The design was simulated until the results converge. Moreover, a Y + check was also performed and the value was discovered not to exceed 500 (Tahani et al., 2016, 464) while flux conservation at the inlet and outlet also produced values below 1% and these were considered to be good (Suchde et al., 2017, 255).

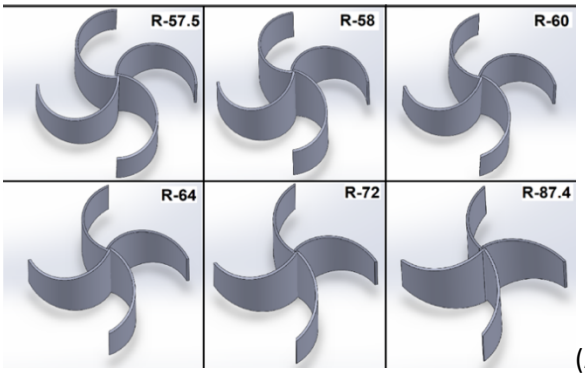

(A)

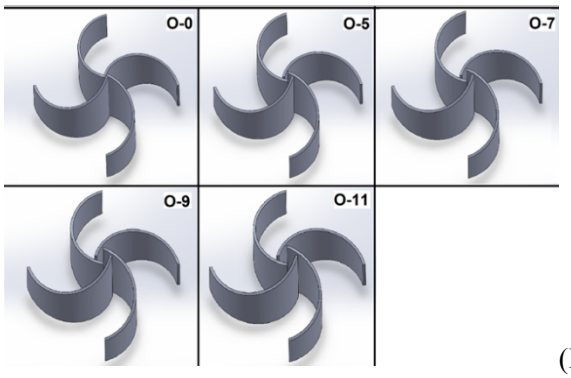

(B)

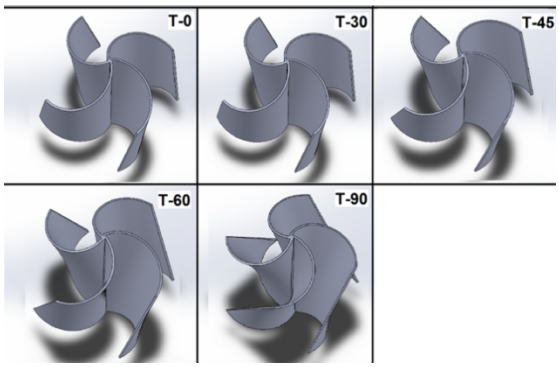

(C)

Figure 11. (A) Variation in the radius of the turbines, (B) Variation in Offset of the turbines, and (C)Variations in Twist of the turbines

Table 2 and Figures 12A and B showed the optimal value of the turbine blade was found at 58 mm radius with 0.5 TSR which produced 2.84 watts of power and torque of 0.099 Nm as indicated in Table 3 while the power coefficient (Cp) was 0.2786. The model of flow and turbulence kinetic energy produced are presented in 11A and B.

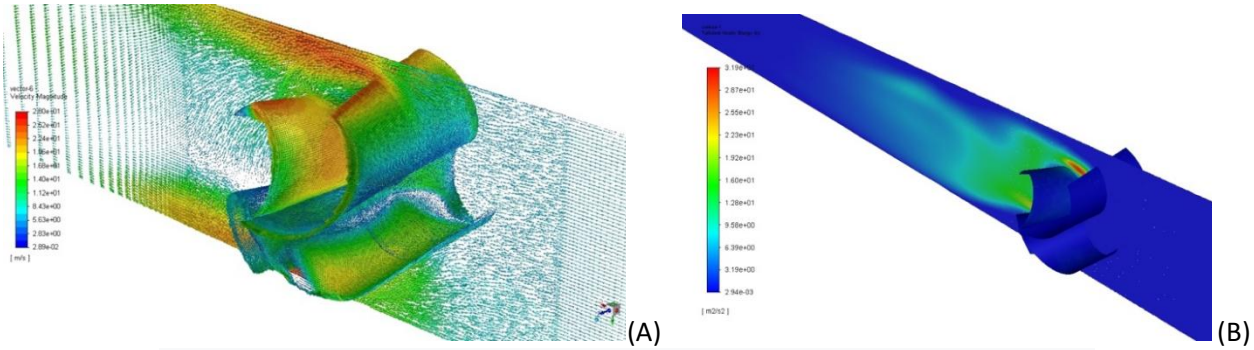

(A) (B)

Figure 12. (A) Vector velocity of wind flow on a 58 mm radius turbine and (B) turbulent kinetic energy in a 58 mm radius turbine

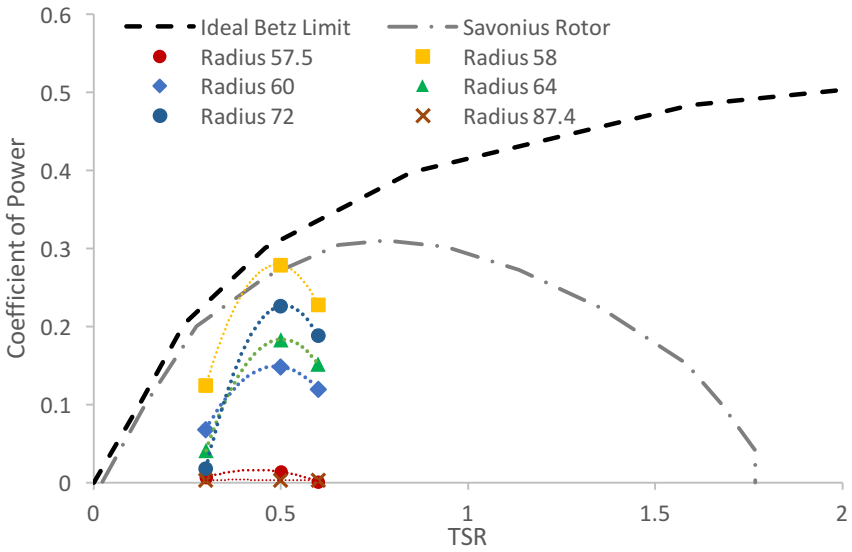

Figure 13. Variants of Turbine Blade Radius

Figure 13 shows the three models with 58 mm, 64 mm, and 72 mm radius, and the highest C_P values have the same flow velocity patterns. It was also discovered that a smaller drag flow was produced when the radius was fixed and this is less favorable for the performance of the turbine. Moreover, a larger radius produced a larger counter-rotating-vortices flow which is also less favorable for performance due to its smaller overlap flow. However, the greatest turbulent kinetic energy distribution in the rotor was found in turbines with the smallest diameter which was 58 mm. This means a larger diameter of the rotor produced the smaller distribution of turbulent kinetic energy as presented in Figure 12B.

Table 3. Variations in Turbine Blade Radius

Radius (mm)	TSR	C_P	Power (Watt)	Torque (N.m)	Y Plus
57.5	0.3	0.0063	0.01414182	0.001355268	83.13049
	0.5	0.01362	0.138701848	0.004817709	132.4085
	0.6	0.00102	0.006001218	0.000208448	112.7113
58	0.3	0.12423	0.278864743	0.026724749	85.26819
	0.5	0.2786	2.837076273	0.098543809	132.8681
	0.6	0.22797	1.338171874	0.04648044	112.3835
60	0.3	0.06798	0.152605393	0.014624799	88.38058
	0.5	0.14847	1.511890424	0.052514429	134.181
	0.6	0.11964	0.702281366	0.02439324	113.8718
64	0.3	0.04071	0.091376894	0.008757022	94.81096
	0.5	0.18333	1.866906431	0.064845656	144.2127
	0.6	0.15165	0.890188959	0.030920075	122.4319
72	0.3	0.01791	0.040192929	0.003851853	102.9334
	0.5	0.22628	2.304257532	0.080036733	156.9534
	0.6	0.18799	1.10346569	0.038328089	133.3397
87.4	0.3	0.00319	0.007153723	0.000685571	111.8106
	0.5	0.00312	0.031819299	0.001105221	184.3163
	0.6	0.00266	0.015604645	0.000542016	156.7907

Table 4 and Figures 14A and B show the optimal value of the turbine blade was produced at 11 mm offset with 0.5 TSR as indicated by the production of 3.05 watts of power, 0.106 Nm of torque, and 0.29918 power coefficient (C_P). The model of flow and turbulence kinetic energy produced are presented in Figure 13B.

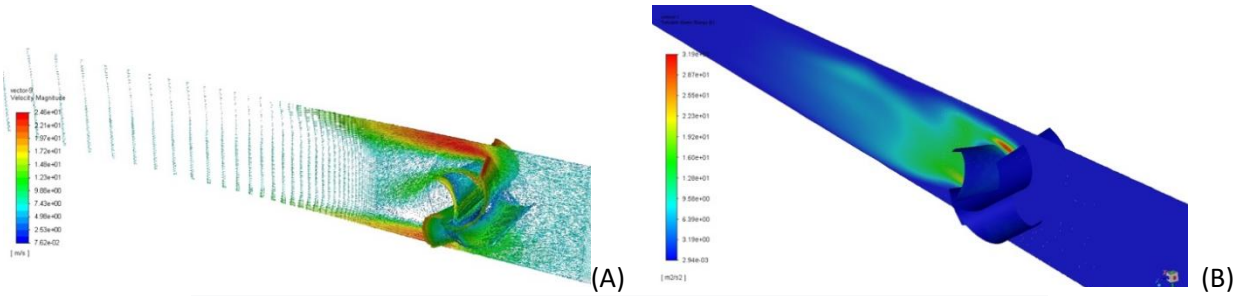

(A) (B)

Figure 14. (A) Vector velocity of wind flow on an 11 mm offset turbine, and (B)turbulent kinetic energy in turbine offset 11 mm

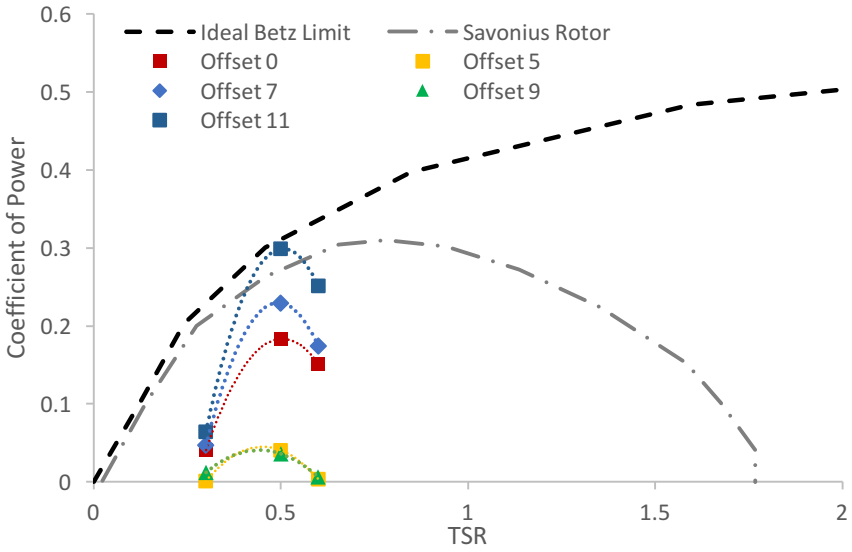

Figure 15. Variants of Turbine Blade Offset (Source: Author)

Figures 15 showed the three models with 11, 7, and 0 offsets with the highest C_P values have almost the same flow velocity patterns. A smaller drag flow was produced when the offset was reduced and this is less favorable to the performance of the turbine and the same was also observed for smaller offsets which caused a greater counter-rotating-vortices flow and smaller overlap flow. Meanwhile, the greater offset of the rotor was observed to cause smaller distribution of turbulent kinetic energy before it increased again.

Table 4. Variations in Turbine Blade Offset

Offset (mm)	TSR	C_P	Power (Watt)	Torque (N.m)	Y Plus
0	0.3	0.04071	0.091377	0.008757	94.81096
	0.5	0.18333	1.866906	0.064846	144.2127
	0.6	0.15165	0.890189	0.03092	122.4319
5	0.3	0.00095	0.002122	0.000203	87.08589
	0.5	0.04072	0.414702	0.014404	132.0764
	0.6	0.00335	0.019688	0.000684	112.0743
7	0.3	0.04683	0.105127	0.010075	84.6218
	0.5	0.22955	2.337588	0.081194	128.1884
	0.6	0.17445	1.023987	0.035567	108.7234
9	0.3	0.01217	0.027321	0.002618	82.36165
	0.5	0.03606	0.367162	0.012753	124.5991
	0.6	0.00611	0.035872	0.001246	105.5825
11	0.3	0.06421	0.144118	0.013811	80.24362
	0.5	0.29918	3.046607	0.105822	121.2431
	0.6	0.250932	1.472946	0.051162	102.7176

Table 4 and Figure 16 show that the optimal value of the turbine blade was at 0-degree twist with 0.5 TSR which produced 4.75 watts of power, 0.165 Nm of torque, and 0.4665 of power coefficient. The model of the flow and turbulence kinetic energy produced is presented in Figure 16B.

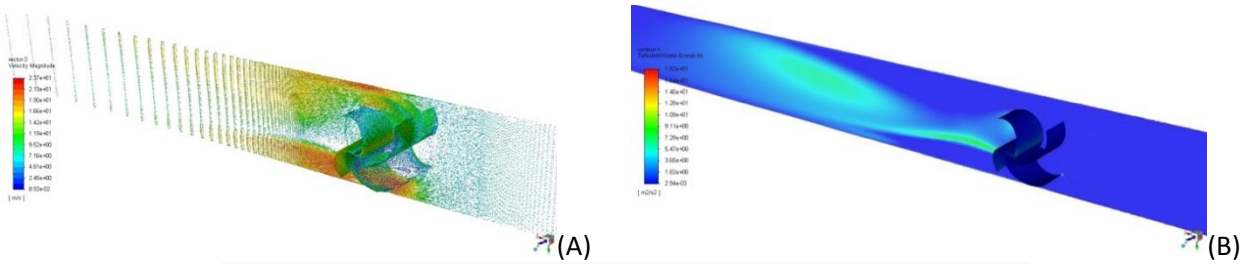

Figure 16. (A)Vector speed of wind flow on turbine twist 0° and (B) turbulent kinetic energy in turbine twist 0°

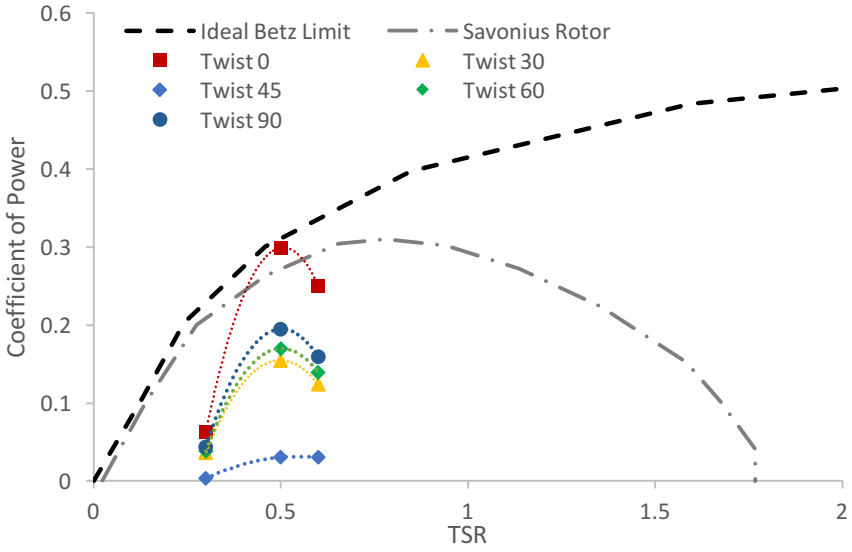

Figure 17. Variants of Turbine Blade Twist

Figure 17 shows the three models 0, 90, and 60 twists with the highest C_P values have almost the same flow velocity patterns. It was discovered that the minimized twist produced a smaller drag flow, and this is less favorable for the performance of the turbine due to its larger counter-rotating-vortices flow. A bigger twist also caused smaller overlap flow which is also considered less favorable and this means a greater twist of the rotor usually leads to a higher distribution of turbulent kinetic energy before the distribution shrinks again.

Table 5. Variations in Turbine Blade Twist

Twist (degree)	TSR	C_P	Power (Watt)	Torque (N.m)	Y Plus
0	0.3	0.06421	0.144118	0.013811	80.24362
	0.5	0.29918	3.046607	0.105822	121.2431
	0.6	0.250932	1.472946	0.051162	102.7176
30	0.3	0.0367	0.082452702	0.00790178	73.73257
	0.5	0.15497	1.578151371	0.054815956	113.7554
	0.6	0.12406	0.728239091	0.025294862	97.44502
45	0.3	0.00339	0.007624782	0.000730714	74.97164
	0.5	0.03044	0.309972006	0.010766655	113.4298

Twist (degree)	TSR	C_P	Power (Watt)	Torque (N.m)	Y Plus
60	0.6	0.03041	0.178473013	0.006199132	96.20094
	0.3	0.03888	0.087283209	0.008364707	72.77678
	0.5	0.1699	1.730730969	0.060115699	112.8925
90	0.6	0.13926	0.817438314	0.028393134	97.33451
	0.3	0.0441	0.099087932	0.009496002	62.60502
	0.5	0.1949	1.984248782	0.068921458	98.08689
	0.6	0.1599	0.938463598	0.03259686	85.9093

The simulation further combined 58 mm radius, 11 mm offset, and 0° twist and the optimal result was also recorded at TSR 0.5 as indicated by 3.046607 Watts power, 0.105822 Nm torque, and 0.29918 Power Coefficient (C_P) produced.

Table 6. Variations in Turbine Blade TSR

TSR	C_P	Power (Watt)	Torque (N.m)	Y Plus
0.3	0.06421	0.144118	0.013811	80.24362
0.5	0.29918	3.046607	0.105822	121.2431
0.6	0.25093	1.472946	0.051162	102.7176

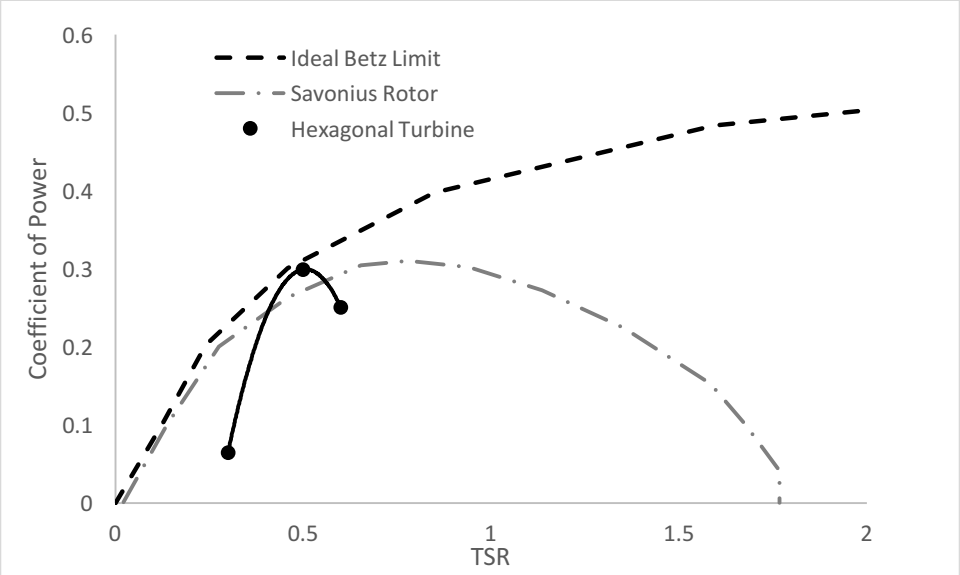

Figure18. Hexagonal Turbine Optimum Model

5. Conclusions

Numerical and CFD simulations were used to analyze the three parts of designing and optimizing the honeycomb module of Savonius micro wind turbine with 4 blades on the second façade building using radius, twist, and offset as the important factors to determine the performance.

The use of 58 mm radius, 11 mm offset, zero-degree twist blade, and 0.5 TSR in one-piece module design of the micro hexagonal wind turbine was found to have produced 3.047 watts of electricity which eliminated the piece modules of honeycomb photovoltaics (as explained in next research) while the optimal Power of Coefficient (C_p) was 0.29918.

The comparison of the Savonius turbine with the Hexagonal Turbine at a TSR of 0.5 showed the Hexagonal Turbine has a lower TSR leading to a smaller U_{inf} requirement. This prediction is associated with the 4 blades used in the design which is more than the Savonius turbine, thereby, causing an increment in the solidity which is very important for the VAWT more than the HAWT. It is also pertinent to note that the high solidity reduces the operating rotation of the wind turbine. Moreover, the Cp value of the Hexagonal Turbine was also found to be higher and close to the Betz limit which is the maximum allowed for wind turbines.

The previous design of Hexagonal Savonius with 4 blades at 90 mm radius as well as unknown offset and twist which was tested in wind tunnel produced only 0.03426 power of coefficient (C_p) and 0.12 watt of electricity. This, therefore, means the numerical and CFD simulation was successfully used to determine the optimal blade radius, offset, and twist to produce renewable energy in hexagonal micro wind turbine architectural building façade.

References

Ahmed, M.M.A., Rahman, A.K.A., Ali, A.H.H., Suzuki, M. (2016). Double Skin Façade: The State of Art on Building Energy Efficiency. *Journal of Clean Energy and Technologies, 4(*1), 84-89.

Arteaga-López, E., Ángeles-Camacho, C., & Bañuelos-Ruedas, F. (2019). Advanced methodology for feasibility studies on building-mounted wind turbines installation in urban environment: Applying CFD analysis. *Energy*, *167*, 181–188. https://doi.org/10.1016/j.energy.2018.10.191

Attoye, D.E., Adekunle, T.O., Tabet Aoul, K., & Hassan, A., (2018). Building Integrated Photovoltaic (BIPV) Adoption: A Conceptual Communication Model for Research and Market Proposals. A Conference Proceeding ASEE Connecticut, USA.

Blackwell, B., Sheldahl, R., & Feltz, L. (1977). Wind Tunnel Performance Data for Two and Three Bucket Savonius Rotors. *Journal of Energy, 2*(3), 160-164.

Cao, X.D., Xilei, D., & Liu, J. (2016). Building Energy-Consumption Status Worldwide and the State-of-the-Art Technologies for Zero-Energy Buildings during the Past Decade. *Energy and Building*, *128*, 1-58.

California Energy Commission (2005). Options for Energy Efficiency in Existing Buildings.

Coyle, E.D., Grimson, W., Basu, B., Murphy, M. (2014). Understading the Global Energy Crisis. Book Chapter part 1: *Reflection on Energy, Greenhouses Gases, and Carbonaceous Fuels*. Purdue University Press.

Daryanto, Y. (2007). *Kajian Potensi Angin untuk Pembangkit Listrik Tenaga Bayu*. Yogjakarta: BALAI PPTAGG – UPT – LAGG.

Dudley, N. (2008). Climate Change and the Energy Crisis. Back to the Energy Crisis – the Need for a Coherent Policy towards Energy Systems. *Policy Matters*, *16*, 12-68.

Elger, D.F., LeBret, B.A., Crowe, C.T., & Robertson, J.A. (2015). *Engineering Fluid Mechanics* (9th ed.).

Ferrari, G., Federici, D., Schito, P., Inzoli, F., & Mereu, R. (2017). CFD Study of Savonius Wind Turbine: 3D model Validation and Parametric Analysis. *Journal of Renewable Energy, 105,* 722-734.

Howells, M., & Roehrl, R.A. (2012). Perspective on Sustainable Energy for the 21th Century (SD21). New York: United Nations Department of Economic Social Affairs, Division for Sustainable Development.

IEA. (2004b). Energy Balances for OECD Countries and Energy Balances for Non-OECD Countries, Energy Statistics for OECD Countries and Energy Statisics for Non-OECD Countries (2004 editions), Paris.

Kumar, A., & Saini, R.P. (2016). Performance Parameter of Savonius Type Hydrokinetic Turbine: A Review. *Journal of Renewable and Sustainable Energy Reviews*, *64*, 289-310.

Manienyen, V., Thambidurai, M., and Selvakumar, R. (2009). Study on Energy Crisis and the Future of Fossil Fuels. *Proceeding of SHEE, Engineering Wing, DDE*., Annamalai University, December 11-12, 2009.

Manwell, J.F., McGowan, J.G., & Rogers, A.L. (2010). *Wind Energy Explained: Theory, Design and Application* (2nd ed.). Wiley.

Mintorogo. D.S., Elsiana, F., & Budhiyantho, A. (2019). Experimental Sustainable Micro Wind Turbines on Second Façade of Buildings. A Research Report. Center for Research, Petra Christian University.

Nowak, D.J., Greenfield, E.J., & Ash, R.M. (2019). Annual Biomass Loss and Potential Value of Urban Tree Waste in the United States. *Urban Forestry & Urban Greening, 46*. 126469. https://www.fs.fed.us/nrs/pubs/jrnl/2019/nrs_2019_nowak_004.pdf. (June, 2020).

Park, J., Jung, H.J., Lee, S.W., Park, J. (2015). A new Building-Integrated Wind Turbine System Utilizing the Building. *Energies*, *8*, 11846–11870.

Rahman, M., Salyers, T.E., El-Shahat, A., Ilie, M., Ahmed, M., & Soloiu, V. (2018). Numerical and Experimental Investigation of Aerodynamic Performance of Vertical-Axis Wind Turbine Models with Various Blade Designs. *Journal of Power and Energy Engineering,* 6(5), 13-14. https://doi.org/10.4236/jpee.2018.65003

Suchde, P., Kuhnert, J., Schröder, S., & Klar, A. (2017). A flux conserving meshfree method for conservation laws. *International Journal for Numerical Methods in Engineering, 112*(3), 238–256. https://doi.org/10.1002/nme.5511

Sutrisno, Mirmanto, H., Sasongko, H., Noor, D. Z. (2015). Study of The Secondary Flow Structure Caused the Additional Forward-facing Step Turbulence Generator. *Advances and Applications in Fluid Mechanics* 18(1), 129-144.
http://dx.doi.org/10.17654/AAFMJul2015_129_144

Simanjuntak, M. E., Prabowo, Widodo, W. A., Sutrisno, Sitorus, M. B. H. (2019). Experimental and Numerical Study of Coal Swirls Fluidized Bed Drying on 10 ° Angle of Guide Vane. *Journal of Mechanical Science and Technology,* 33, 5499-5505.

https://doi.org/10.1007/s12206-019-1042-2.

Tahani, M., Babayan, N., Mehrnia, S., & Shadmehri, M. (2016). A Novel Heuristic Method for Optimization of Straight Blade Vertical Wind Turbine. *Energy Conversion and Management*, *127*, 461–476. https://doi.org/10.1016/j.enconman.2016.08.094

Wenehenubun, F., Saputra, A., & Sutanto, H. (2015). An experimental study on the performance of Savonius wind turbines related with the number of blades. *Energy Procedia*, *68*, 297–304. https://doi.org/10.1016/j.egypro.2015.03.259

6. Paper accepted (11-11-2021)

Journal of Asian Architecture and Building Engineering - Decision on Manuscript ID JAABE2101027EE.R1

External
Inbox

Journal of Asian Architecture and Building Engineering <onbehalfof@manuscriptcentral.com> Thu, Nov 11, 2021, 3:17 PM
to me

11-Nov-2021

Dear Dr. Mintorogo:

It is a pleasure to accept your manuscript entitled "Harvesting Renewable Energies through Innovative Kinetic Honeycomb Architectural Facades: The Mathematical & CFD Modeling for Wind Turbine Design Optimization" for publication in the XXX 20XX issue of the Journal of Asian Architecture and Building Engineering.

Thank you for your fine contribution. On behalf of the Editors of the Journal of Asian Architecture and Building Engineering, we look forward to your continued contributions to the Journal.

Sincerely,

Xilin Lu
Chief Editor, Journal of Asian Architecture and Building Engineering

Editor(s)' Comments to Author:

Associate Editor: 1
Comments to the Author:
(There are no comments.)

Field Editor: 2
Comments to the Author:
(There are no comments.)

Field Editor: 3
Comments to Author::
(There are no comments.)

Reviewer(s)' Comments to Author:

Reviewer: 1

Comments to be returned to author(s)
The revision had addressed the previous reviews of the manuscript.

7. License Agreement (14-11-2021)

Journal of Asian Architecture and Building Engineering - Please complete your author agreement

External

Inbox

authoragreement@taylorandfrancis.com Sat, Nov 13, 2021, 9:36 AM

to me

Taylor & Francis Group plc

Your Author Publishing Agreement (APA) with Taylor and Francis

Attention: Danny S. Mintorogo

Hello,

In order to publish your article, "Harvesting Renewable Energies through Innovative Kinetic Honeycomb Architectural Facades: The Mathematical & CFD Modeling for Wind Turbine Design Optimization", we ask that you complete your Author Publishing Agreement. Please click the link below (or copy the URL into your browser) to launch our online Author Publishing Agreement portal. The process should take only a few minutes. In most cases, you will receive immediate notice that your agreement is accepted and will be able to download a copy of it for your records.

Please do not reply to this email. If you need immediate assistance concerning your article, please instead contact TABE-production@journals.tandf.co.uk.

Thank you.

Start »

https://authoragreement.taylorandfrancisgroup.com/Start/69f0d98b-b762-4e00-b288-7602a7764207

LICENSE AGREEMENT

This is a licence agreement under which you, the author, retain copyright in your article, and grant Architectural Institute of Japan, 26-20, Shiba 5-chome, Minato-ku, Tokyo, Japan 108-8414, Architectural Institute of Korea, 203 Architecture Center, 87 hyoryeong-ro, Seocho-Ku, Seoul 137-843, Korea and Architectural Society of China, No.9, Sanlihe Road, Beijing, China 1000835 (hereinafter 'the Society') to allow us and our publisher Informa UK Limited registered in England under no. 1072954 trading as Taylor & Francis Group, Registered Office: Mortimer House, 37–41 Mortimer Street, London W1T 3JH (hereinafter 'Taylor & Francis') a non-exclusive licence to publish your article, including abstract, tables, figures, data, and supplemental material hosted by our publisher, as the Version of Record in the Journal on an Open Access basis under a Creative Commons Attribution License (CC BY) http://creativecommons.org/licenses/by/4.0/ subject to the Terms & Conditions set out below.

ARTICLE TITLE ('Article'):	Harvesting Renewable Energies through Innovative Kinetic Honeycomb Architectural Facades: The Mathematical & CFD Modeling for Wind Turbine Design Optimization
ARTICE DOI:	10.1080/13467581.2021.2007102
AUTHOR(S):	Danny S. Mintorogo, Aris Budhiyanto, Feny Elsiana, Fandi D. Suprianto, Sutrisno Sutrisno
JOURNAL TITLE ('Journal'):	Journal of Asian Architecture and Building Engineering
JOURNAL ISSN:	1347-2852

In consideration of the publication of the Article, you hereby grant with full title guarantee all rights of copyright and related rights in the above specified Article as the Version of Scholarly Record which is intended for publication in all forms and all media (whether known at this time or developed at any time in the future) throughout the world, in all languages, for the full term of copyright, to take effect if and when the Article is accepted for publication in the Journal.

- I confirm that I have read and accept the full terms of the Journal's Article Publishing Agreement including the Terms & Conditions.
- I confirm the article will be made available under the following access and use licence. I have read and understood the terms of this licence: Creative Commons Attribution License (CC BY).
- I confirm that I agree to assume responsibility for any applicable payment of the Article Publishing Charge.
- I confirm I grant the Society the rights to publish my article on an Open Access basis, in all forms and all media (whether known at this time or developed at any time in the future) throughout the world, including the right to translate the article into other languages, create adaptations, summaries or extracts of the article or other derivative works based on the article and the right to sub-license all such rights to others subject to the Terms & Conditions set out below, to take effect if and when the article is accepted for publication. If a statement of government or corporate ownership appears above, that statement modifies this assignment as described.
- I confirm that I have read and accept my author warranties.
- I confirm that I have read and agree to comply with Taylor & Francis' policy on publishing ethics

GRANT OF PUBLISHING RIGHTS

Signed and dated: 14 November 2021

THIS FORM IS A LEGALLY BINDING DOCUMENT. WE RECOMMEND THAT YOU RETAIN A COPY OF IT AND CONSULT A LEGAL ADVISOR IF YOU HAVE ANY QUESTIONS.

LICENSE TO PUBLISH: TERMS & CONDITIONS

DEFINITION

1. Your article is defined as comprising (a) your Accepted Manuscript (AM) in its final form; (b) the final, definitive, and citable Version of Record (VoR) including the abstract, text, bibliography, and all accompanying tables, illustrations, data, and media; and (c) any supplemental material hosted by our publisher. This assignment and these Terms & Conditions constitute the entire agreement and the sole understanding between you and us ('agreement'); no amendment, addendum, or other communication will be taken into account when interpreting your and our rights and obligations under this agreement, unless amended by a written document signed by both of us.

TAYLOR & FRANCIS' RESPONSIBILITIES

2. If deemed acceptable by the Editors of the Journal, we shall prepare and publish your article in the Journal. We may post your accepted manuscript as free-to-access in advance of the formal publication of the Version of Record (VoR). We shall publish the VoR in the Journal on an Open Access basis, viz., to be made freely available online with no subscription fee or article-pay-to-view fee or any other form of access fee or any publication embargo being applied,. We reserve the right to make such editorial changes as may be necessary to make the article suitable for publication or as we reasonably consider necessary to avoid infringing third-party rights or breaching any laws; and we reserve the right not to proceed with publication for whatever reason.
3. If before publication we reasonably consider that the article should not be published, on the advice of our legal advisors, we may decline to publish the article, in which case we will refund you any Article Publishing Charge you have paid.
4. If after publication we reasonably consider that the article should be retracted or removed from our website, on the advice of our legal advisors, for example, because of a breach in your Author Warranties, we may retract and withdraw it, and in such case shall be under no obligation to refund you any Article Publishing Charge you have paid.
5. If we do not receive payment of the applicable Article Publishing Charge after six (6) weeks, we reserve the right to rescind the Open Access status of your article and to publish it on an exclusive licence basis.

YOUR RIGHTS AS AUTHOR

6. These rights are personal to you, and your co-authors, and cannot be transferred by you to anyone else. You assert and retain the following rights as author(s):
    i. The right to re-use your own work on a commercial or non-commercial basis, and in any way permitted under the Creative Commons Attribution License (CC BY), including but not limited to, translation, adaptation, and resale.
    ii. The right to be identified as the author of your article, whenever and wherever the article is published, such rights including moral rights arising under § 77, Copyright, Designs & Patents Act 1988, and, so far as is legally possible, any corresponding rights we may have in any territory of the world.
    iii. The right to retain patent rights, trademark rights, or rights to any process, product or procedure described in your article.
    iv. The right to post and maintain at any time the Author's Original Manuscript (AOM; your manuscript in its original and unrefereed form; a 'preprint').
    v. The right to post and maintain at any time your 'Author's Original Manuscript (AOM), i.e., the unpublished version of the article created by you prior to peer review; the AM; and the article in its published form as supplied by us as a digital eprint on your own website for personal or professional use, or on your institution's network or intranet or website, or in a subject repository or network, with the acknowledgement: 'The Version of Record of this manuscript has been published and is freely available in <JOURNAL TITLE> <date of publication> http://www.tandfonline.com/<Article DOI>.'

WARRANTIES MADE BY YOU AS AUTHOR

7. You warrant that:
    i. All persons who have a reasonable claim to authorship are named in the article as co-authors including yourself, and you have not fabricated or misappropriated anyone's identity, including your own.
    ii. You have been authorized by all such co-authors to sign this agreement as agent on their behalf, and to agree on their behalf the priority of the assertion of copyright and the order of names in the publication of the article.
    iii. The article is your original work, apart from any permitted third-party copyright material you include, and does not infringe any intellectual property rights of any other person or entity and cannot be construed as plagiarizing any other published work, including your own published work.
    iv. The article is not currently under submission to, nor is under consideration by, nor has been accepted by any other journal or publication, nor has been previously published by any other journal or publication, nor has been assigned or licensed by you to any third party.
    v. The article contains no content that is abusive, defamatory, libellous, obscene, fraudulent, nor in any way infringes the rights of others, nor is in any other way unlawful or in violation of applicable laws.
    vi. Research reported in the article has been conducted in an ethical and responsible manner, in full compliance with all relevant codes of experimentation and legislation. All articles which report in vivo experiments or clinical trials on humans or animals must include a written statement in the Methods section that such work was conducted with the formal approval of the local human subject or animal care committees, and that clinical trials have been registered as applicable legislation requires.

vii. Any patient, service user, or participant (or that person's parent or legal guardian) in any research or clinical experiment or study who is described in the article has given written consent to the inclusion of material, text or image, pertaining to themselves, and that they acknowledge that they cannot be identified via the article and that you have anonymized them and that you do not identify them in any way. Where such a person is deceased, you warrant you have obtained the written consent of the deceased person's family or estate.

viii. You have complied with all mandatory laboratory health and safety procedures in the course of conducting any experimental work reported in your article; your article contains all appropriate warnings concerning any specific and particular hazards that may be involved in carrying out experiments or procedures described in the article or involved in instructions, materials, or formulae in the article; your article includes explicitly relevant safety precautions; and cites, if an accepted Standard or Code of Practice is relevant, a reference to the relevant Standard or Code.

ix. You have acknowledged all sources of research funding, as required by your research funder, and disclosed any financial interest or benefit you have arising from the direct applications of your research.

x. You have obtained the necessary written permission to include material in your article that is owned and held in copyright by a third party, which shall include but is not limited to any proprietary text, illustration, table, or other material, including data, audio, video, film stills, screenshots, musical notation and any supplemental material.

xi. You have read and complied with our policy on publishing ethics.

xii. You have read and complied with the Journal's Instructions for Authors.

xiii. You have read and complied with our guide on peer review.

xiv. You will keep us and our affiliates indemnified in full against all loss, damages, injury, costs and expenses (including legal and other professional fees and expenses) awarded against or incurred or paid by us as a result of your breach of the warranties given in this agreement.

xv. You consent to allowing us to use your article for marketing and promotional purposes.

GOVERNING LAW

8. This agreement (and any dispute, proceeding, claim or controversy in relation to it) is subject to English law and the parties hereby submit to the exclusive jurisdiction of the Courts of England and Wales.

THIRD PARTY ACCESS & USAGE TERMS & CONDITIONS FOR OPEN ACCESS CONTENT RIGHTS ARE GIVEN AT http://www.tandfonline.com/page/terms-and-conditions